Chapter 4

Measurement and Numerical Modeling of Mechanical Properties of Polyurethane Foams

Michal Petrů and Ondřej Novák

Additional information is available at the end of the chapter

http://dx.doi.org/10.5772/intechopen.69700

Abstract

This chapter focuses on determination of mechanical properties of polyurethane foams applied in automotive industry and medicine. These materials have strong nonlinear viscoelastic behavior that is time dependent. A comprehensive description of their characteristics is very tough and difficult. Mechanical properties can to some extent be studied using mathematical models that need to be verified with measurements. This chapter describes selected mathematical relationships, rheological models, and also numerical simulations that can approximately describe mechanical properties. Mechanical properties of polyurethane foam are influenced by internal and external structure, shape and size of the cells, filling volume, and properties of the used polymer. Studied mechanical properties are contact pressures, stress distribution, and the dependence of stress on the strain rate.

Keywords: PU foam, stiffness, dynamical tests, contact pressure, FEM

1. Introduction

Mechanical properties of polyurethane foams compressed during fast and dynamic states are among others affected by a friction of the cellular structure and the air contained in the cells [1–3]. However, this does not significantly contribute to a compressive force in certain range of the deformation as reported in Ref. [4]. On behavior under compression, loading a significant influence has mechanical and physical properties of the PU foam such as a geometry, thickness, or density, which is explained by [5]. A decrease of the thickness of the comfort stuff from polyurethane foam brings desired weight reduction, but it reduces the total damping, and on the contrary, the total stiffness increases. Therefore, the trend in automotive industry has been a development of low density polyurethane foams with lower bulk density having better

mechanical properties under compression than commonly used PU foams [2]. Another solution that can change mechanical properties is a vertical layering of polyurethane foams having different physical and mechanical properties. But it does not bring an expected improvement of characteristics corresponding with a composite behavior [6, 7], which may be due to the fact that only the layering of polyurethane foams does not bring the desired synergistic effect as stated by Ref. [8]. Also, a significant improvement in energy savings and vibroisolation characteristics or other parameters such as a permeability of PU foam is not achieved. The improvements are reflected only in reduced values of contact pressures from the load body [9]. The mechanical behavior of polyurethane foams can be considered substantially non-linear, with a large viscoelastic deformation, relaxation, and recovery of the structure.

2. Analysis of the properties of selected PU foam samples

Mechanical, chemical, and physical properties together with the experimentally identified structural properties of samples of different densities ρ_{PU} PU foams have been published in Refs. [1, 2, 5]. The structure of the polyurethane foam is formed by a chemical process polyaddition from alcohols with two or more hydroxyl groups and isocyanates. Isocyanate reacts with water to form carbon dioxide that creates cell structure of polyurethane foam. According to the applied type of ingredients and their ratio, PU foam can be divided into soft, moderately stiff, rigid, or hard. The flexibility of the cell structure is among others dependent on its density $\rho_{PU} = weight/volume$, which for comfort application is in the range from 10 to 100 kg m^{-3}. Samples of polyurethane foams can be characterized with low-permeable envelop, which arises as a consequence of heat removal from polyurethane with a mold wall. The internal cell structure is characterized by a distribution curve of the cell diameters, and it is significantly more porous, which, for porous structure, can be expressed by a dimensionless quantity Ψ in accordance with Eq. (1). The relationship describes the ratio of the polyurethane structure volume and total volume of structure, which is important for obtaining of the parameter named as a packing density. A number of porous cells and the connecting edges (edge connecting air cells) are significantly influenced by the diameter of cells as indicated in Ref. [1]. He also states that the structure of PU foam created by combining of individual cells is the macroscopic homogeneous system and regardless of the variability of cell diameters, and therefore it can replace a continuum or rheological models. In terms of a deformation mechanism, the behavior of foams can be characterized by the following aspects: during foam compression, the air escapes from the cell, the cell walls are bent, and from a certain phase, cell walls are in a contact with specific friction. During unloading, the air is sucked again into the structure. Therefore, for the fast compression of the cellular structure of the foam, the mechanical properties depend especially on the amount of air and the breathability of porous cells and thus on strain rate $\dot{\varepsilon}(t)$. Already in 1970 in Ref. [10], it was published that the rate of air cells has an influence on the value of an energy dissipation $\vartheta(t)$, which PU foam can absorb. From the viewpoint of the mechanical properties, polyurethane foams are nearly isotropic viscoelastic materials. It has been published in 1987 by Ref. [11]. They state that during tri-axial test, wherein the sample is simultaneously loaded in three main directions of the basic coordinate system (X, Y, and Z), approximately same course of

http://dx.doi.org/10.5772/intechopen.69700

the loading curves is obtained. They differ only in constant. As a result, deformation/strain ε in the main axis of the load and a volumetric deformation γ can be expressed with Eqs. (2) and (3). The results of analysis of the structure of PU foam samples with dimensions of 100 × 100 × 40 mm, which were numbered 1–6, are shown in **Table 1**. Air volume in the analyzed samples reached 96.5 ± 0.5%, wherein the parameter of the packing density Ψ was from 0.033 to 0.034. It is due to the density of pure polyurethane polymer (for the comfort stuff, it is from 1200 to 1500 kg m^{-3}). Depending on the increasing amount of polyurethane in the PU foam sample, the air volume decreases. This fact can be illustrated with a parametric graph (**Figure 1**).

$$\Psi = \frac{V_{polym}}{V_{air}}, \tag{1}$$

where Ψ [−] is the parameter of the packing density of PU foam, V_{polym} is the volume of PU foam [m^3], and V_{air} [m^3] is volume of the air.

Sample	Density [kg m^{-3}]	Areal weight [g m^{-2}]	Air content [%]	Ψ [−]	Average size of cells (inner structure) [μm]	Average size of cells (outer structure) [μm]
1	48 ± 0.01	1920 ± 0.40	96.0 ± 0.80	0.032	544 ± 37	687 ± 51
2	51 ± 0.26	2045 ± 5.20	96.5 ± 0.92	0.034	446 ± 43	562 ± 48
3	50 ± 0.16	2003 ± 3.20	96.6 ± 0.67	0.033	478 ± 26	601 ± 63
4	47 ± 0.33	1887 ± 3	96.8 ± 0.70	0.031	593 ± 52	690 ± 39
5	50 ± 0.12	2002 ± 0.40	96.6 ± 0.27	0.034	462 ± 27	613 ± 53
6	49 ± 0.39	1966 ± 7.13	96.7 ± 0.22	0.033	455 ± 45	625 ± 38

Table 1. Parameters of tested PU samples.

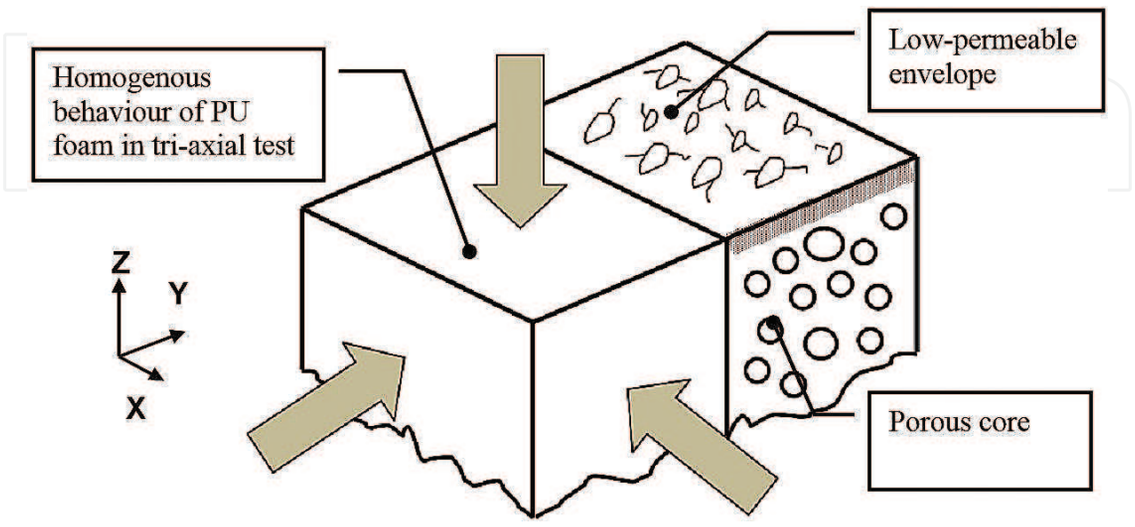

Figure 1. Characteristic structure of PU foam.

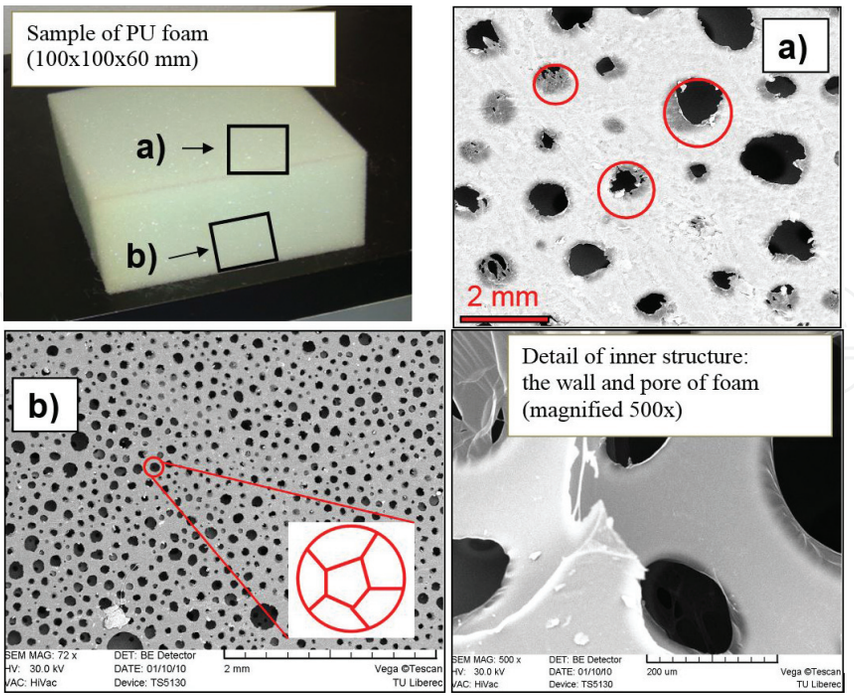

Figure 2. (a) Inner structure (low-porous envelop). (b) Inner structure of PU foam with characteristic shape of cell (left) and detail of inner structure (right).

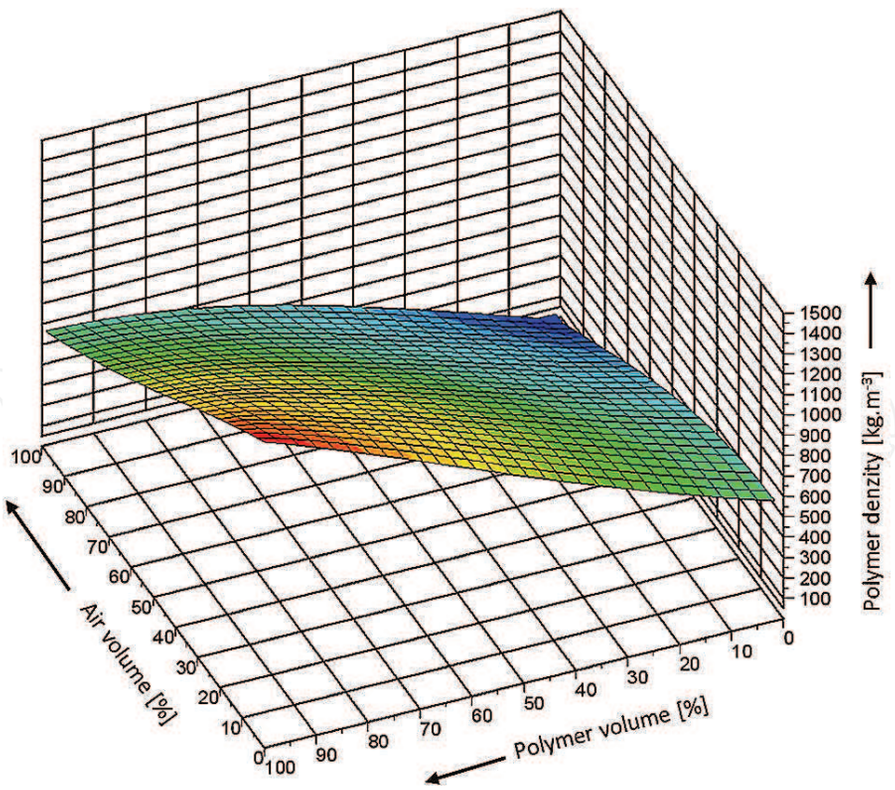

Figure 3. The volume of air and material in the structure of polyurethane foams depending on the specific weight of pure polymer.

http://dx.doi.org/10.5772/intechopen.69700

$$\Gamma = \frac{\Delta V}{V_0} = \frac{V_0 - V_{comp}}{V_0} = \frac{\left(V_{air} + V_{polym}\right) - V_{comp}}{\left(V_{air} + V_{polym}\right)} = 1 - \Phi, \tag{2}$$

$$\varepsilon = \frac{L_0 - \delta}{L_0} = 1 - \left[1 - \frac{V_0 - V_{comp}}{V_0}\right]^{1/3} = 1 - [1 - \gamma]^{1/3}, \tag{3}$$

where $\Gamma[-]$ is total volume strain of PU foam, V_{comp} [m^3] is compressed volume, V_0 [m^3] is undeformed volume, V_{polym} [m^3] is volume of the polymer in PU foam, V_{air} [m^3] is volume of air in cells, Φ [−] is ratio of compressed and uncompressed volume, ε [−] is strain, δ [mm] is value (length) of compression, and L_0 [mm] is origin undeformed length (**Figures 2** and **3**).

3. Measurement of properties of selected samples during static compression

Mechanical properties of selected samples of PU foams show a stress dependent on the strain rate, which is accompanied by a change of stiffness. The stiffness of the sample can be experimentally determined as a slope of the tangent of the force depending on compression or deformation. The most significant change of K is in the initial phase (area no. 1, **Figure 13**). The material damping η_t is a mechanical variable that is difficult to measure. It can be approximated for example by energy dissipation in a hysteresis curve. But it should be understood that the obtained values will vary depending on the strain rate and the geometry of the loading body. Generally, two foams with the same density may not have the same stiffness. Comparative parameter may be contact pressures and the transmission characteristic that the value of the resonant frequency determines. There are numerous of methodologies describing the mechanical properties of PU foam, but they are not standardized. Therefore, own measurement methodology was designed and implemented for a measurement of properties under static and dynamic compression.

3.1. Determination of mechanical properties of samples of PU foams under static compression

For obtaining mechanical properties of selected materials under static or quasi-static compression, the measurements were made on samples compressed with rigid steel plate with dimensions of 200 × 200 × 50 mm. The specimen having areal dimension 100 × 100 mm was placed on the rigid support. Samples change mechanical properties with the thickness that is reflected in the changing of the stiffness and damping. These properties have measured on the PU foam with thickness 60, 40 and 20 mm (sample No. 3). For the tests (Figure 4) an universal testing machine Labortech 2.050 was used. A tension load cell with loading capacity 1 kN was placed on a moving part of the measuring device. For the measurement, up to 50% deformation in accordance with the standard DIN 54 305 was applied. This standard is used for quasi-static compression tests of bulky fibrous structures, PU foam, and similar materials. The strain rate was set 60 mm min^{-1}. After deformation, achieving the unloading phase up to 0% deformation

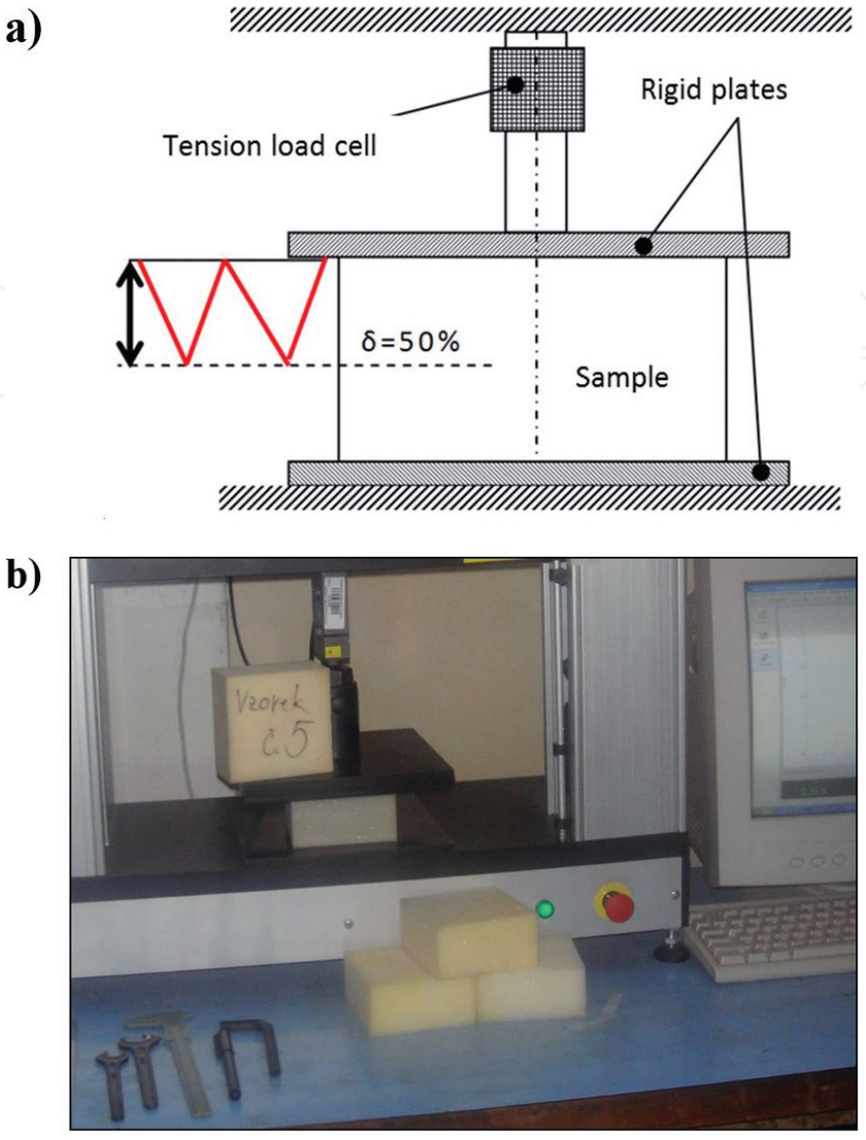

Figure 4. Determination of mechanical properties of samples of polyurethane foams during static compression: (a) scheme, (b) realization of the measurement.

follows. This represents one cycle that is four times repeated. A loading signal has a triangular wave shape. During the test, the force depending on compression is recorded. The results of PU foam samples with different thickness are shown in **Figure 5**. The results have confirmed that with decreasing thickness, the force required to compression of the sample to the desired deformation increases. It is also seen that between loading and unloading cycle is a hysteresis, and between first and second cycles, a significant loss of force occurs (relaxation of the material). The stiffness of samples was measured at the 5th cycle (**Figure 6**). The stiffness of samples with thickness 60 and 40 mm in the range between 30 and 50 % exhibits a difference about 20 % (2000 N/m), while highest force at 50% deformation differs only about 30 N. A sample with a thickness of 20 mm exhibited an increase in strength of 80 N in comparison with a sample thickness of

http://dx.doi.org/10.5772/intechopen.69700

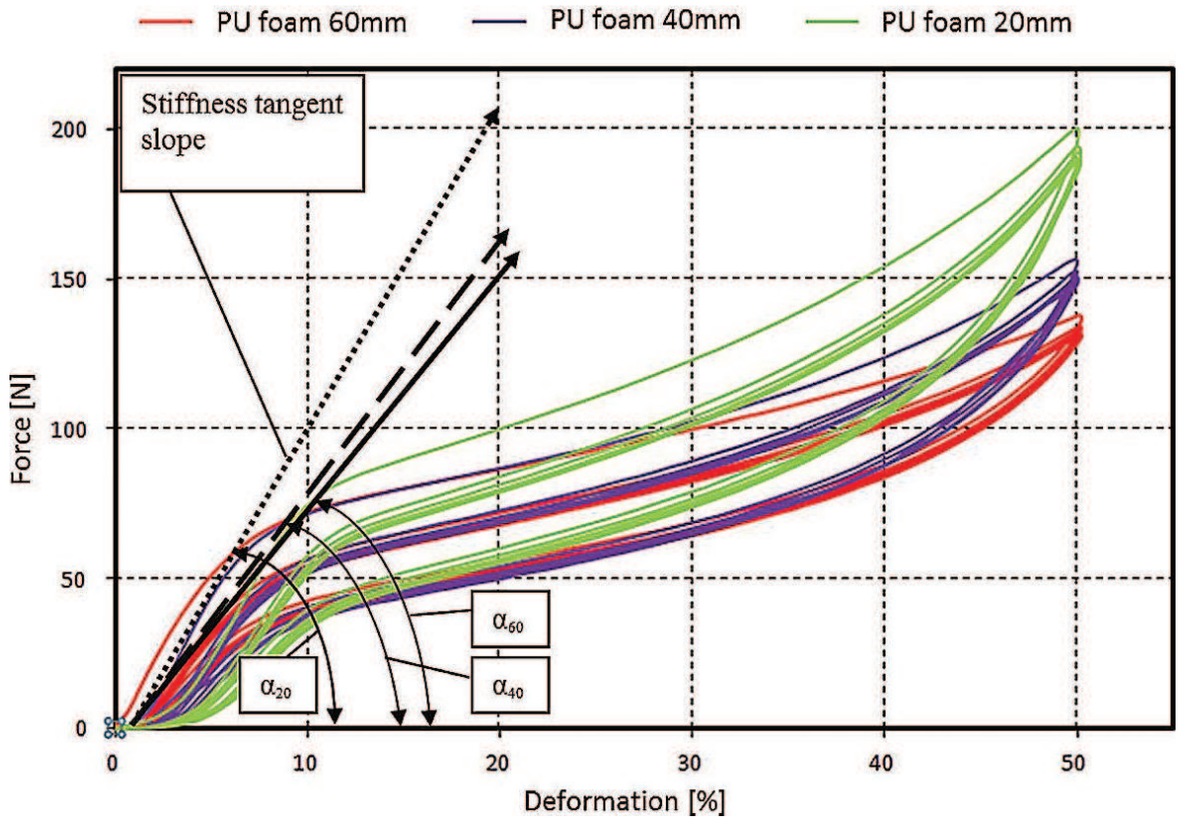

Figure 5. Dependence of force on the deformation of PU foam samples with dimensions 100 × 100 × 60, 40 and 20 mm during cyclic compression.

60 mm, and increase in strength of 50 N in comparison with a sample having a thickness of 40 mm. However, the stiffness of the sample having a thickness of 20 mm compared with the samples having a thickness of 40 and 60 mm increased about approximately 11,000 N/m. There can be applied the inequality $\alpha_{60} < \alpha_{40} < \alpha_{20}$, that describes tangent slope of initial stiffness of the cellular structure of a given thickness. It can be concluded that the targeted reduction in the thickness of the polyurethane foam (the idea of new seat and back car seats design) is not useful for the quality of the seating. It is not suitable especially for safety reasons. For example, currently manufactured headrests, where the structure of comfortable filler is made of PU foam having the thickness less than 20 mm exhibit at high strain rate significant hardening of the structure [3].

3.2. Determination of mechanical properties of PU samples during dynamic compression

Mechanical properties during dynamic compression relate to the ability of the material to dampen incoming vibrations with a given frequency and amplitude. It is caused by the reorganization of the structure, in this instance cellular, in which entering mechanical energy is being transformed to heat in a short time interval. Great amount of the dissipated mechanical energy $\vartheta(t)$ that was

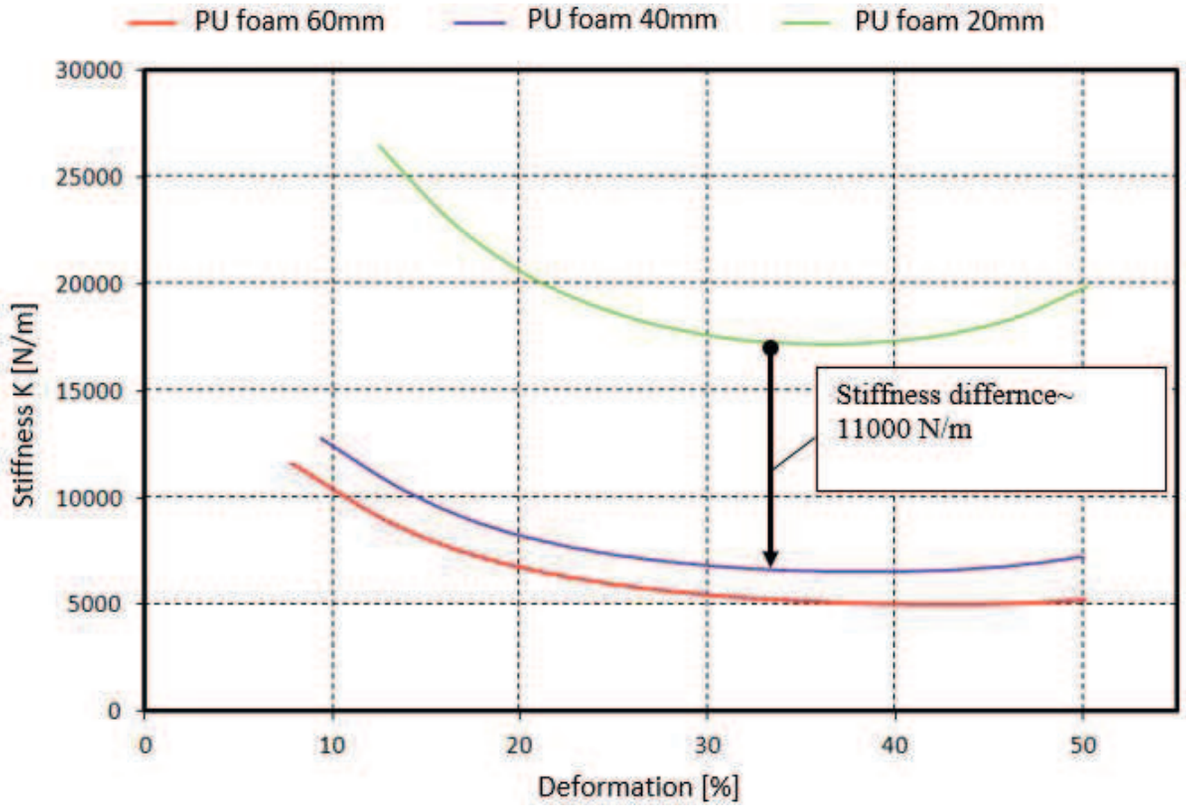

Figure 6. Dependence of stiffness on the deformation of PU foam samples with dimensions 100 × 100 × 60, 40 and 20 mm.

described by Eq. (23) is proportional to the area of hysteresis curve that describes the relation between tension and the relative deformation during one cycle of harmonic stress. Generally, with viscoelastic structures, it is true that in the harmonic excitation, the structure stress $\sigma(t)$ and deformation $\varepsilon(t)$ change in time, while $\varepsilon(t)$ has certain phase delay to the applied stress $\sigma(t)$, which is defined by Eqs. (4) and (5). Phase shift $\phi(t)$ between the tension and relative deformation lies during the harmonic excitation in the interval $\phi(t) \in (0, \pi/2)$.

$$\sigma(t) = \sigma \cdot \cos(\omega \cdot t + \phi) = \sigma \cdot \cos\phi \cdot \cos(\omega \cdot t) + \sigma \cdot \sin\phi \cdot \cos(\omega \cdot t + \pi/2) \tag{4}$$

$$\varepsilon(t) = \varepsilon \cdot \cos(\omega \cdot t), \tag{5}$$

Eq. (4) describing time dependency of the tension during harmonic compression can be further described in Eq. (6) expressing components of the dynamic module of the material structure.

$$\sigma(t) = E_P^{'} \cdot \varepsilon \cdot \cos(\omega \cdot t) + E_P^{''} \cdot \varepsilon \cdot \cos(\omega \cdot t + \pi/2), \tag{6}$$

where $E_P^{'}$ is a real component of the dynamic flexibility module describing durability properties of the material, and $E_P^{''}$ is imaginary component of the dynamic flexibility module describing dissipation of energy (loss module). Both modules are described by Eqs. (7) and (8), from which it is possible to obtain complex dynamic module E_P^D according to Eq. (9).

$$E_P^{'} = \frac{\sigma_0}{\varepsilon_0} \cdot \cos\phi, \tag{7}$$

$$E_P^{''} = \frac{\sigma_0}{\varepsilon_0} \cdot \sin\phi, \tag{8}$$

$$E_P^{'} = \frac{\sigma_0}{\varepsilon_0} \cdot \cos\phi, \tag{9}$$

where E_P^D is a complex dynamic module and i represents imaginary component.

To obtain mechanical properties during dynamic compression of the selected PU foams, measurements with 100 × 100 × 40 mm samples were conducted. All observed properties from these measurements can be summarized in these points:

- Determining the mechanical properties of selected samples with dynamic compression against a rigid plate without the initial deformation.
- Determining the mechanical properties of selected samples with dynamic compression against a rigid plate with the initial deformation.

3.3. Determining the mechanical properties of selected samples with dynamic compression against a rigid plate without the initial deformation

The experiment took place in the hydrodynamic laboratory (HDL). The measuring device was comprised of a hydraulic cylinder with an attached contraption to insert the sample. The contraption consists of two vertical supporting tubes put on the circular plate that were connected by a crosspiece from the top. In the middle of the crosspiece, an immovable tube pole was attached, with a 0.5 kN sensor placed on it. The sample was put between the upper and lower rigid plates. The arrangement of the conducted experiment is described in **Figure 7**. Input excitation harmonic signal (stationary periodical) was defined by Eq. (10). This signal is suitable for more than a study and experimental comparison of the material samples of different structures, because it is a base signal for the comparison and optimization of competent car seats [6].

$$y_{(z)} = A_{(z)} \cdot \sin(\omega t), \tag{10}$$

where $y_{(z)}$ is a defined cylindrical lift, $A_{(z)}$ is the input amplitude, and $\omega = 2\pi f$ is an angular velocity.

There are two possible approaches to define the input excitation of the hydraulic cylinder:

1. **Measurement with frequencies comprised in one input file** (one measurement with gradual change of the frequency value)
2. **Measurement with initial constant frequency value** (gradual measurement)

Measurements of the selected samples were conducted according to the method number 2—*measurement with a constant initial frequency value*. In total, seven measurements with a gradually rising frequency f were conducted, starting from 0.5, 1, 2, 3, 4, 5, and 8 Hz with constant

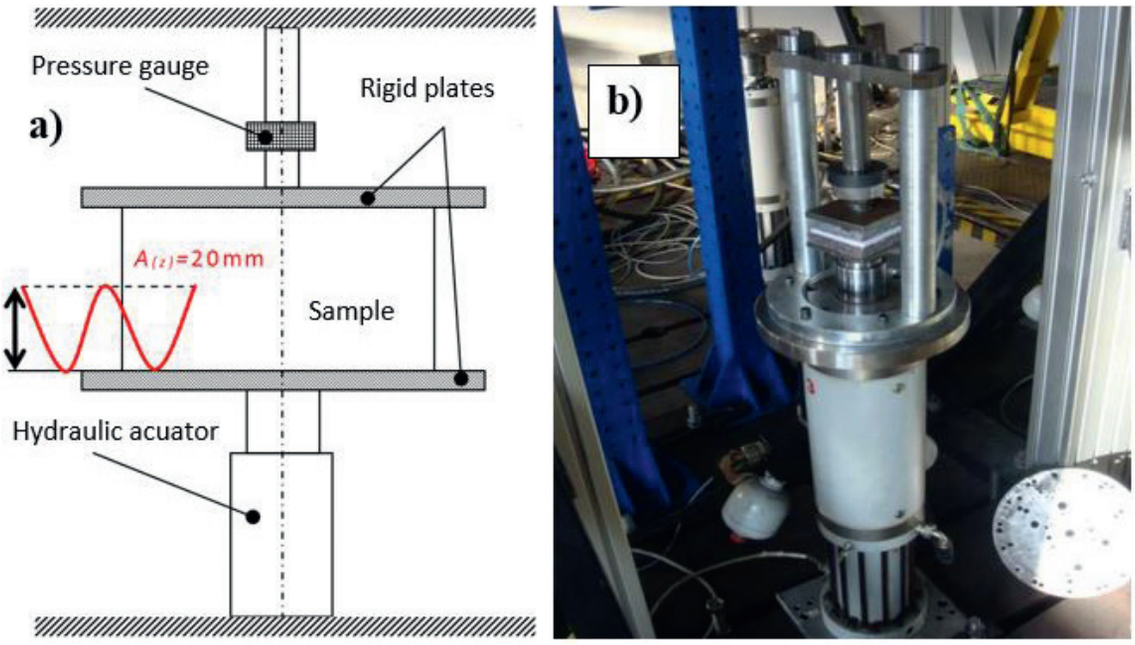

Figure 7. Determination of mechanical properties of samples of polyurethane foams during dynamic compression: (a) scheme, (b) realization of the measurement.

value of the amplitude $A_{(z)} = 20\ mm$ (i.e. up to 50% deformation) for the evaluation of five consecutive cycles. The difference of the harmonic course of a given input frequency is described in **Figure 8**, describing how the rising frequency value also raises the value of a phase shift (oscillation) of the hydraulic cylinder. Measurements were repeated three times. The resultant courses of the tested PU foam sample for individual frequency values during the fifth cycle are shown in **Figure 9**. The resultant courses of the dependence between pressure forces applied on the PU foam samples that were compressed against a rigid plate without the initial deformation for selected frequency values, which were 0.5, 2, and 4 Hz, are presented in **Figure 11**. The order of experiment where initial deformation is applied is shown in **Figure 10**.

The results of harmonic compression without the initial deformation in the fifth cycle of the PU foam sample (**Figure 9**) show that the change in frequency changes hysteresis force dependence on the pressure and relief. Looking at the PU foam sample, it is apparent that increasing frequency value 0.5, 2, and 4 Hz also increases the value of the force necessary to compress the material, but on the other hand starts dropping for frequencies 5 and 8 Hz. Maximum force value necessary to compress the PU foam sample was 191 N during 4 Hz frequency, while frequency 5 Hz slightly decreases the force value to 182 N and frequency 8 Hz requires only 165 N. This shows that the cell structure of the PU foam sample changes mechanical properties with the speed of deformation and change in frequency. It is apparent from the results that the PU foam sample changes its properties based on the speed of deformation, while the main influence can be seen in the presence of air in the foam structure. The air is not capable of getting back into the structure during unloading after reaching a certain strain rate; therefore, its influence is not as significant and the force value also decreases during compression.

http://dx.doi.org/10.5772/intechopen.69700

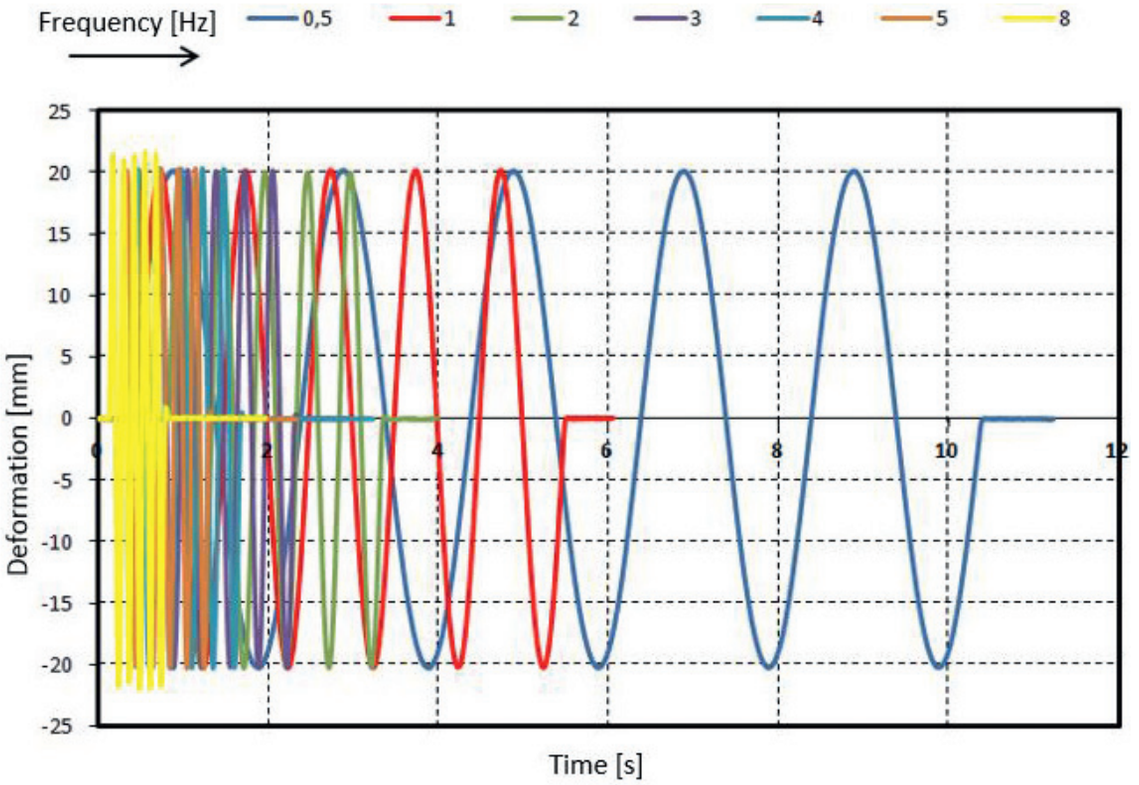

Figure 8. Input harmonic signals for measuring of dynamically compressed samples without initial deformation.

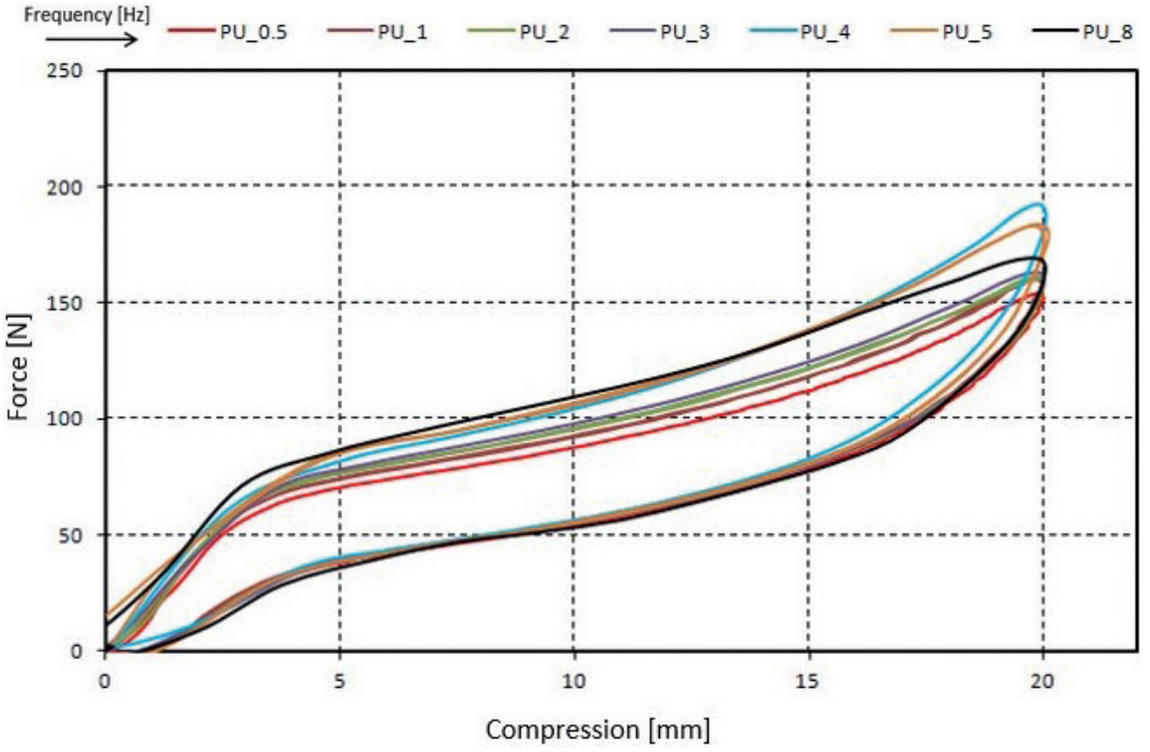

Figure 9. Dependence of force on deformation of dynamically compressed samples without initial deformation.

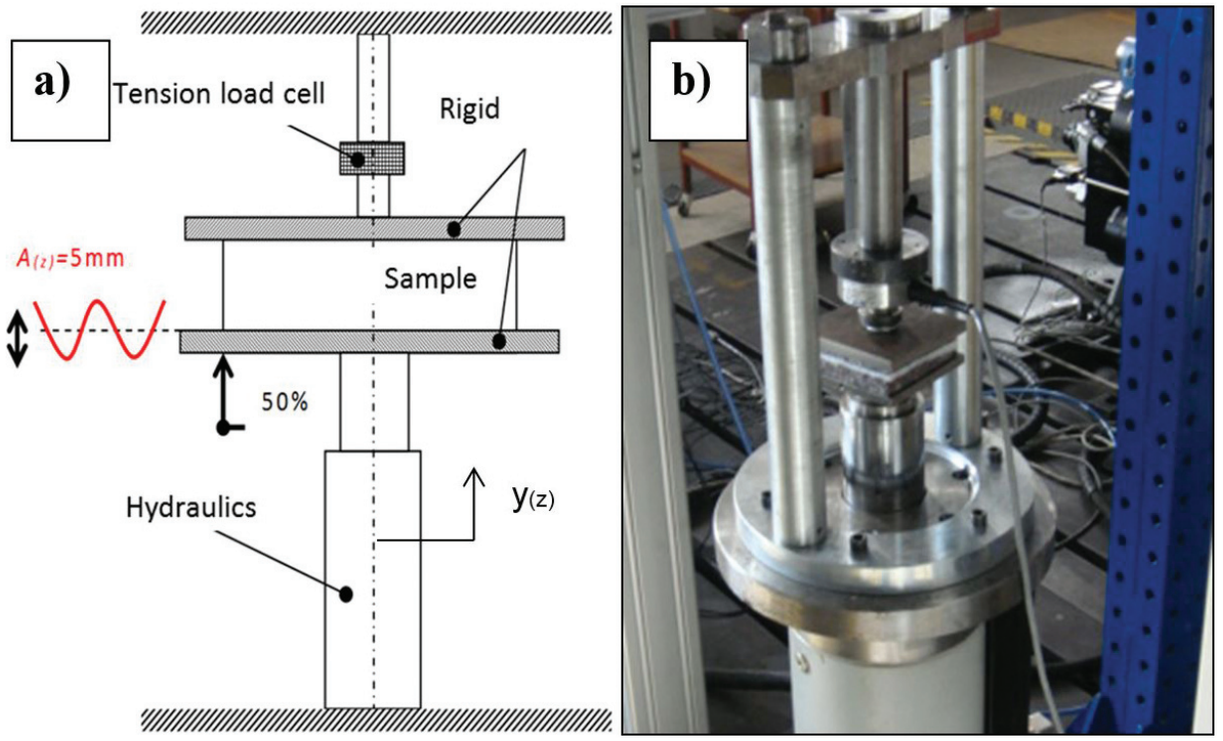

Figure 10. Determination of mechanical properties of samples of polyurethane foams during dynamic compression with initial deformation: (a) scheme, (b) realization of the measurement.

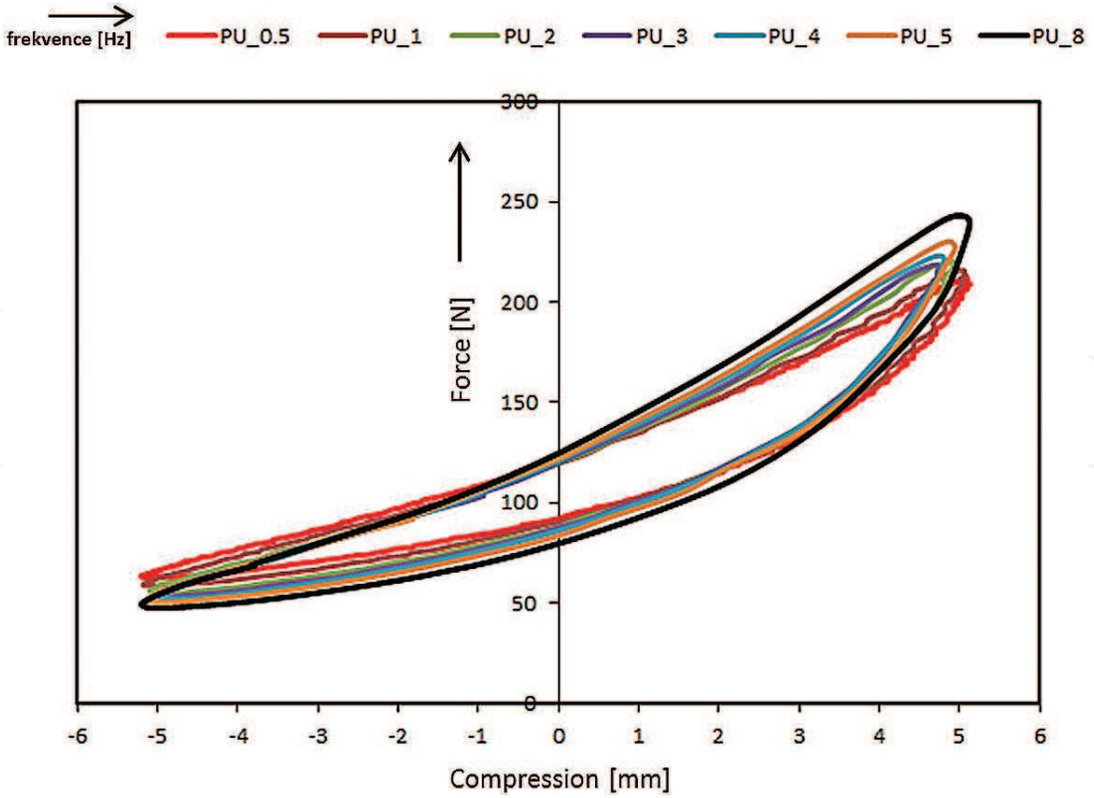

Figure 11. Dependence of force on deformation of dynamically compressed samples with initial deformation.

3.4. Determining the mechanical properties of selected samples with dynamic compression against a rigid plate with the initial deformation

The experiment with chosen samples was conducted 60 min after the first measurement, a long enough time necessary to relax the tested sample. The only difference in measurement was that the tested sample was compressed by the upper rigid plate by 20 mm to its initial 50% deformation. After the initial compression, seven measurements with gradually rising frequency f were conducted, from 0.5, 1, 2, 3, 4, 5, and 8 Hz but with the amplitude at $A_{(z)} = 5\ mm$ for five repeating cycles. The arrangement of the experiment is shown in **Figure 10**. The resultant courses of the tested PU foam sample for individual frequency values during the fifth cycle are shown in **Figure 9**.

Results for the PU foam sample with initial 50% deformation in the fifth cycle of the repeated compression (**Figure 11**) show that the change in frequency also increases the force necessary to compress the material that reaches maximum 246 N and frequency of 8 Hz. This is different, compared to the dynamic measurement of the sample without the initial deformation, because beginning with 5 Hz value, the necessary compression force began to drop. The courses also have a very similar character while comparing samples with different frequency of 0.5, 2, 4, and 8 Hz, which creates so-called "banana curve" shown in **Figure 11**. While comparing the courses during 8 Hz frequency, a dynamic ratio i_d expressing the ratio between the maximum force value and minimum force value of the force relief during compression in the PU foam samples is $i_d = 4.86$ (min 50 N and max 243 N). The higher the value of the dynamic ratio between maximum and minimum force, the faster the material recovers, because there is a greater energy return to recover the material. From the maximum force value necessary to compress the tested sample during the dynamic measurement, it is apparent that the value is higher than during a static compression; therefore, the rigidity of the sample increases. It is possible to determine the dynamic flexibility module E_P^D is greater than static flexibility module E_P^S.

3.5. Measuring the relaxation of the chosen material samples

Also, it is important to compare the mechanical properties during a long-term compression. As it was stated, the cellular structure of the PU foam becomes more supple under constant pressure, and the increase in deformation grows $\varepsilon(t_2)|_{\sigma=konst} > \varepsilon(t_1)$, i.e. the structure "melts," or during the constant deformation, $\varepsilon = konst.$ relaxes and the tension gradually decreases $\sigma(t_2)|_{g=konst} < \sigma(t_1)$. This is true in general for all materials with viscoelastic properties. According to Refs. [1, 6], it is more advantageous to measure the relaxation of material for the evaluation of mechanical properties, because the "melting" of the structure during the constant compression is minimal and almost negligible (the significance grows during long-term measurements—weeks, months—in high temperatures). Comparison of the compressed samples was conducted to evaluate the relaxation of material. The experiment was conducted on the same device just as during the static testing (**Figure 4**). The relaxation properties were compared for the PU foam samples $100 \times 100 \times 40$ mm. The observed properties obtained from these measurements can be summarized in the following points:

- determining the relaxation of the chosen samples compressed by the rigid plate into the constant deformation value.
- determining the relaxation module for the chosen samples.

3.6. Determining the relaxation of the chosen samples compressed by the rigid plate into the constant deformation value

The sample was compressed by the rigid plate into the constant value atduring 10, 25, 50, and 65% deformation, while measuring the material response to the compression during 3600 s. Resultant courses of the sample force response dependence to time are shown in **Figure 12**.

The resultant comparison of the course of relaxation of the PU foam sample shows minimum relaxation during low deformation values (10 and 25%); on the other hand, there was an apparent decrease in force over time during 50–65% deformation. The PU foam sample had a decrease in force of 34 N during 65% deformation (initial force value was 118 N and the final force value was 84 N). The drop in force overtime can be converted to the decrease in tension over time, which can then express the values of the relaxation modulus *G(t)* according to Eq. (14) describing the decrease in tension in the material structure in a time sequence. Values *G(t)* for each deformation differed in the PU foam sample. This can be explained by the cellular structure with low initial deformation of 10% having greater rigidity and cellular structure with greater initial deformation having less air in its structure. In fact, the structure closes and the permeability decreases, and therefore the air cannot return to the structure. Relaxation module values for the tested samples are shown in **Table 2**.

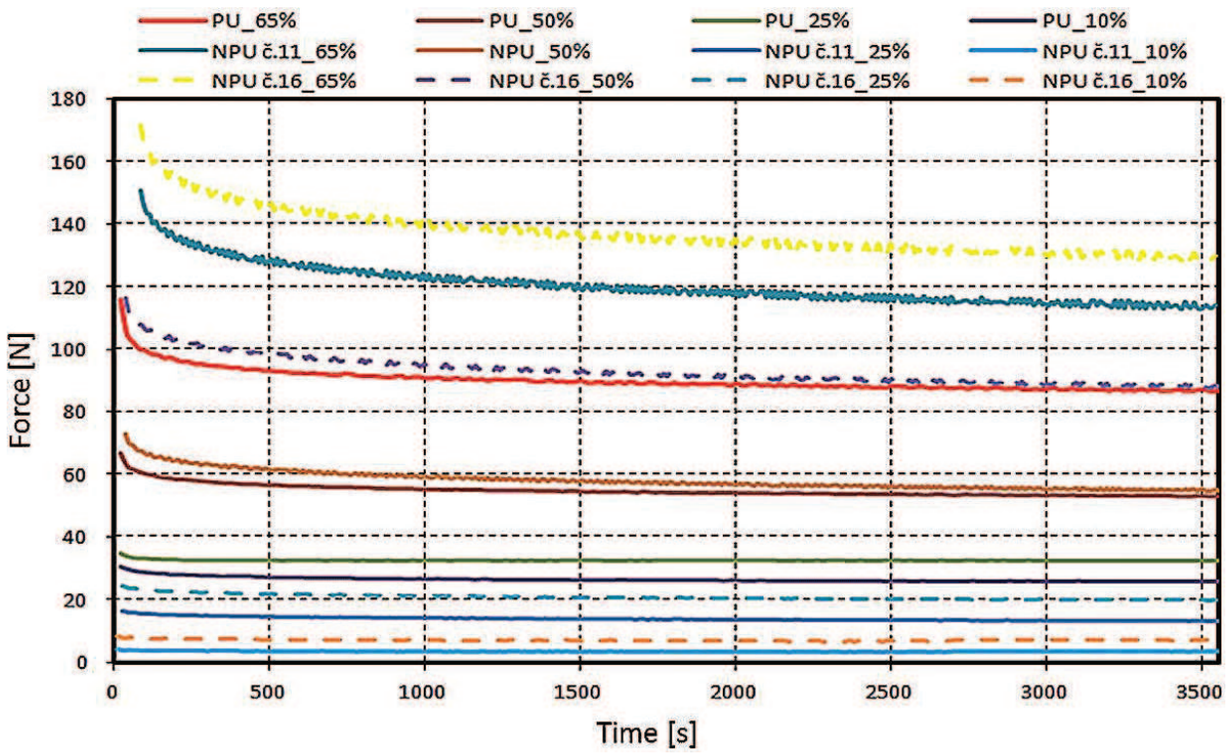

Figure 12. Comparison of relaxation experiment of PU foam.

http://dx.doi.org/10.5772/intechopen.69700

Time *t* [s]	500	1000	1500	2000	2500	3600	Deformation [%]
G(t) [KPa] of PU foam	0.280	0.270	0.265	0.240	0.240	0.240	10
	0.132	0.128	0.126	0.126	0.126	0.126	25
	0.112	0.108	0.106	0.102	0.100	0.099	50
	0.143	0.137	0.134	0.131	0.128	0.128	65

Table 2. Results of relaxation modulus $G(t)$.

3.7. Mathematic-physical description of mechanical behavior of PU foam samples

Mechanical properties of the PU foam samples have a non-linear course during compression. This is a viscoelastic behavior with great, almost returnable, transformation, in the order of 92 ± 3% [12]. During the force relief on the foam, the hysteresis loop manifests, based on the volume weight, rigidity K, and damping coefficient η_t with gradual relaxation of the cell structure, that is more significant during the quasi-static compression than dynamic, among others [6, 12]. The inability of rapid recovery after the deformation also materializes. During the compression, the non-linear behavior of PU foam sample is characterized by three areas: first, initial solidification; second, steady course of deformation during the minimum gain in absolute tension; and third, final and significant solidification of the cell structure. Characteristic course of tension in the dependence on the transformation of the tested PU foam sample is shown in **Figure 13**.

The graphic course shown in **Figure 13** characterizes nonlinear dependence of tension on the transformation, gained during the experimental measurement of the PU foam sample number 3 (**Table 1**) compressed to 98 ± 2% transformation. The sample number 3 had characteristic **area 1** —lasting up to ∼12 ± 3% transformation, which was given by the elastic, almost linear, course with a steep onset of the tension caused by initially fast solidification of the cellular structure, where the inclination of the curve is dependent on the strain rate. **Area 2** can be set for the range of 15–50 ± 5% transformation, where so-called plateau takes place (even temporary stabilization) meaning the absolute increase in tension depending on the transformation is minimal. In the **area 3**, approximately from 60 ± 7 up to 92 ± 3% deformation begins a steep exponential course caused by the final compression of the structure (the structure starts to almost mash). Already, in the year 1969, Rush [13] published analytical model closely describing the behavior of the compressed PU foam. The author based his assumptions on the constitutive equation describing the response of the material after compression, that is characterized by a constant module of flexibility E, the size of deformation transformation ε, and the compression function $\Lambda(\varepsilon)$, that can be described by Eq. (11), where E presents module of foam flexibility, ε is deformation, and $\Lambda(\varepsilon)$ is compression function.

$$\sigma = E \cdot \varepsilon \cdot \Lambda(\varepsilon), \tag{11}$$

Constitutive Eq. (11) was improved upon by Schwaber and Meinecke [14] in 1971 and by Nagy et al. [15] in 1974 by the functional dependence of variable flexibility modulus E on the strain rate $\dot{\varepsilon}$, which is described by Eqs. (12) and (13). These relations can be used to determine immediate rigidity in the structure, because the weight of the structure $m(\varepsilon, \dot{\varepsilon})$ and the flexibility

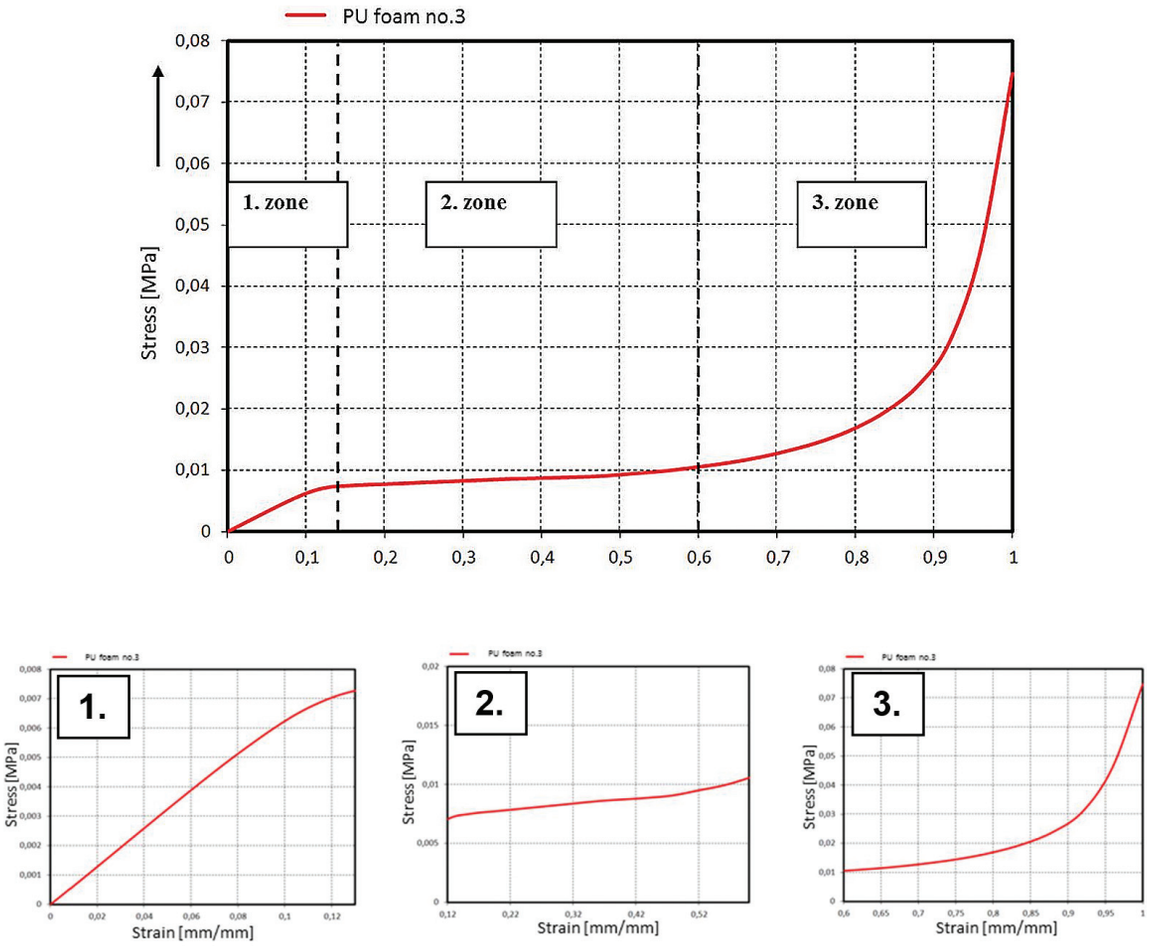

Figure 13. Nonlinear dependence of stress of PU foam sample (top), and the characteristic courses in three main areas (bottom).

modulus $E(\dot{\varepsilon})$ are variable and depend on the immediate state of the deformation or transformation ε.

$$\sigma = E(\dot{\varepsilon}) \cdot f(\varepsilon) \cdot \varepsilon, \tag{12}$$

$$\sigma = m(\varepsilon, \dot{\varepsilon}) \cdot f(\varepsilon), \tag{13}$$

where $f(\varepsilon)$ describes polynomial function describing the course during compression, $m(\varepsilon, \dot{\varepsilon})$ is the weight of the structure that is variable on deformation ε and the strain rate $\dot{\varepsilon}$.

Characteristic properties of the PU foam sample during compression are influenced mostly by the size of the deformation $\varepsilon(t)$ but also time t that takes to compress the cellular structure. Related to this is a physical effect called creep (thinning the structure); in other words, the structure of the PU foam becomes suppler under constant pressure and the deformation increases $\varepsilon(t_2)|_{\sigma=konst} > \varepsilon(t_1)$. Similarly behaves the structure during relaxation of the material—during constant deformation $\varepsilon = konst$ (for example, repeated cyclic compression up

http://dx.doi.org/10.5772/intechopen.69700

to 50% transformation and the material fatigue), the tension gradually decreases. It is possible to describe this physical effect by the value of the relaxation modulus $G(t)$ (14) described by the relation between acting tension $\sigma(t)$ and a constant $G(t)$ deformation $\varepsilon = konst$. In Ref. [1], it is stated that increasing deformation of the PU foam sample decreases the value $G(t)$ where a setting of relaxation modulus values materializes during long-term test for values of small and large deformations as stated in **Figure 14**. This effect is caused by viscoelasticity of the material (this does not have to be true in all viscoelastic materials, and it even can be reversed).

$$G(t) = \frac{\sigma(t)}{\varepsilon_{konst}} \tag{14}$$

Mechanical properties of the PU foam are further determined by the temperature T. Authors in [16] already included the influence of temperature T in the analytical model and consecutive constitutive relation is further described by Eq. (15). The relation character (15) was further improved in Ref. [17] by material constants a, b reflecting even the strain rate $\dot{\varepsilon}$ in relation to morphology of the foam, described by Eq. (16). Authors already establish constants in the model, which statistically describe the frequency of air bubbles in the structure. It is necessary to mention that the significant influence of temperature on the foam behavior happens according to the experience of the producers only in foams used to fill the comfort layers of

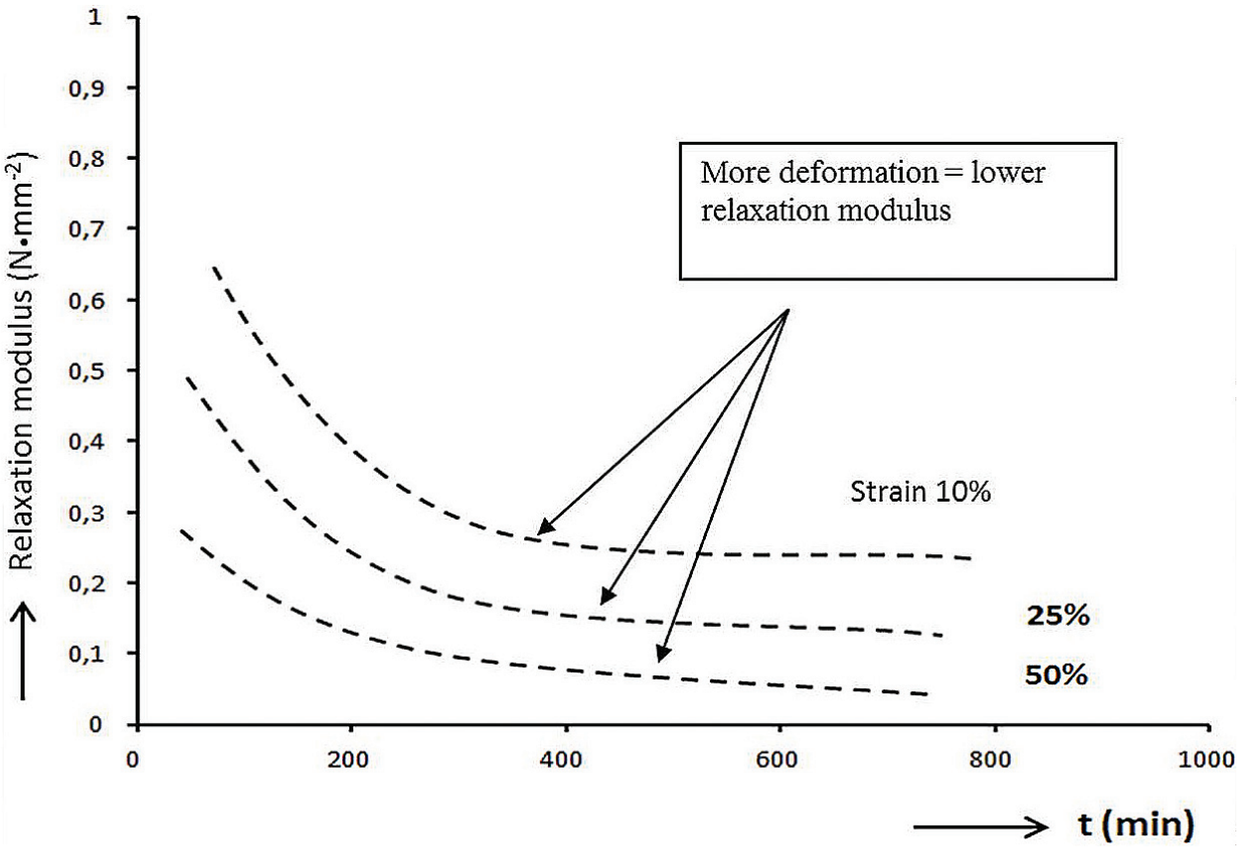

Figure 14. Relaxation modulus of viscoelastic material depending on time.

the car seats during high deviations from the room temperature (for example extreme cold −40°C or on the other hand extremely high temperatures above 70°C).

$$\sigma = h(T, \dot{\varepsilon}) \cdot g(\rho) \cdot f(\varepsilon), \tag{15}$$

$$\sigma = \sigma_0(\varepsilon) \cdot h(T) \cdot \left[\frac{\dot{\varepsilon}}{\dot{\varepsilon}_0}\right]^{a+b\tau} \tag{16}$$

where $h(T, \dot{\varepsilon})$ expresses a step function related to the temperature T and the change in the strain rate $\dot{\varepsilon}$, $g(\rho)$ is experimentally set value related to the structure density, and a, b are material constants $(a, b \geq 1)$.

Viscoelastic behavior of the PU foam can be significantly described using rheological models, i.e. Refs. [8, 14, 16, 17]. Rheology is a science investigating mostly changes in tension σ and transformations in relation to time t and the strain rate $\dot{\varepsilon}$. It stems from the transformation of continuum and therefore does not investigate the structure mechanics (structure morphology and typology, number of air bubbles) compared to the previous relations. Models are created via system of connections of various combinations of Hook elastic elements (springs) and Newton viscose components (damper). They allow for approximate description of non-linear behavior of materials structures including PU foam, by linear components in a various number and combination. It is possible to also study the relaxation and material creep from the obtained relations from the rheological models. The advantage of rheological models is mostly independence on material models in the finite element method programs. In the wide range of publications concerning modeling of PU foam, i.e. Refs. [6, 8], a one-dimensional Kelvin or Maxwell rheological model was used. Authors often mention good congruence of the resultant dependencies of the rheological model in comparison with experimental measurements. Complex cellular structure of the PU foam causes more complicated rheological behavior, where deformation always contains part of elastic, viscose, or sometimes permanent deformation. From the refining values of these one-dimensional rheological models, we can consecutively obtain their n-parameter expansion, shown in **Figure 15**.

It is possible to create rheological model, which will be getting significantly (in limit) close to the experimentally measured data, by a mutual composition and combination of n-parametric Kelvin and N-parametric Maxwell model, better said by a various number of compounded Hook and Newton elements. According to such model, it will be possible to create a corresponding mathematical expression describing mechanical properties of the PU foam sample, especially the dependence of force/compression or tension/transformation or also dampening and elastic properties (rigidity coefficient K and a dampening coefficient η_t on the immediate transformation). This can be achieved by a rheological model according to **Figure 16**. This is a modified n-parametric Tucket model. This model shows practically three characteristic areas. The first part is comprised of a sum of m-number of springs (while $m < n$), which describes initial solidification characteristic by an elastic deformation. The second part represents an n-parametric Kelvin model, comprised by a sum of m—parallel-connected springs and dampers, which describe the delayed viscoelastic deformation. The third part is then characterized by a sum of m—number of dampers (while $m < n$), describing final remaining deformation after tension ceases to be applied. The advantage of this model is

http://dx.doi.org/10.5772/intechopen.69700

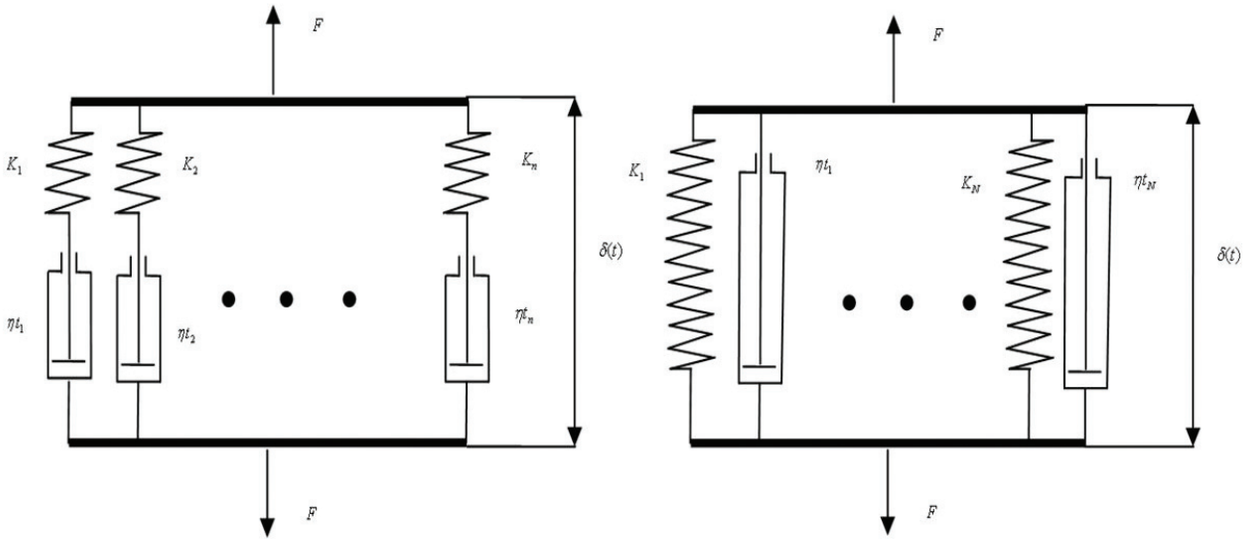

Figure 15. *N*-parametric rheological models: Maxwell model (left) and Kelvin model (right).

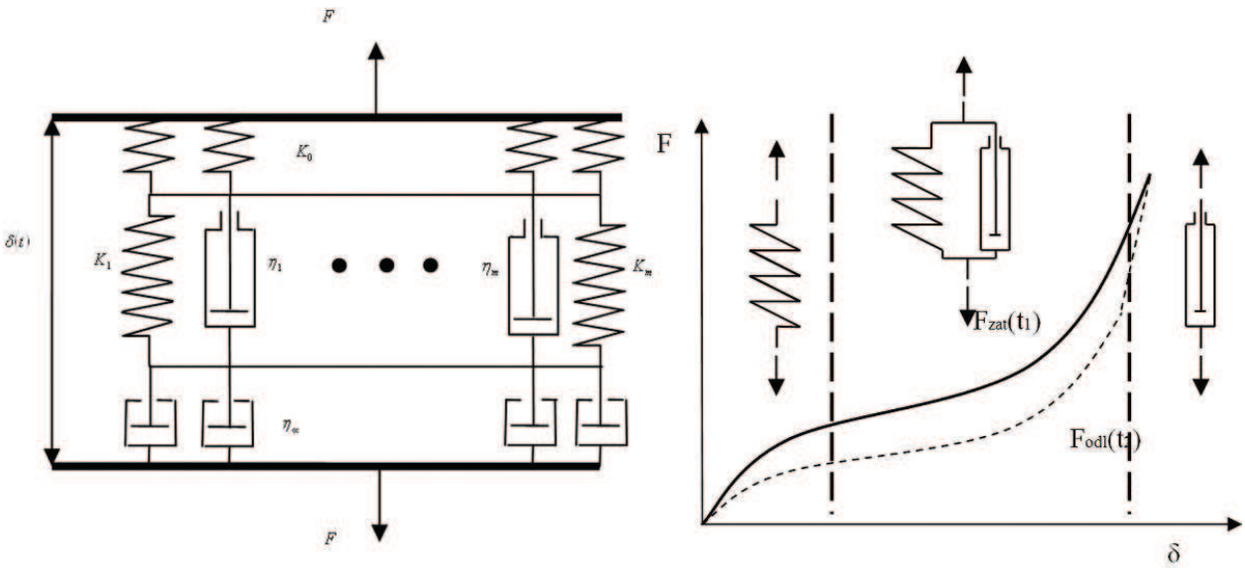

Figure 16. *N*-parametric Tucket model allowing description of nonlinear behavior of PU foam.

mainly the fact that the faster the deformation is supposed to happen, the greater the inhibition effect of the viscoelastic element; therefore, greater force must be applied to achieve desired deformation. The model therefore describes the behavior of viscoelastic material that increases resistance to compression of the applied force by an inner viscose medium. After the force ceases to be applied (final value of compression $\delta|_{\tau=\max}$), the deformation stays maintained in a limit moment $\varepsilon(t) \equiv \delta|_{t=0}$, and after some time, recovery follows.

According to the following rheological model (**Figure 16**), we can construct a corresponding mathematical expression of the compressed PU foam sample by the Eqs. (17)–(24) describing the dependence of the force on compression, for example, rigidity, dampening, or creep suppleness.

$$\sum_{i=1}^{m}\left(K_{PU}(\tau_1)\cdot\overline{\delta}(\tau_1)+\frac{d}{d\tau_1}\left(\eta_{tPU}(\tau_1)\overline{\delta}(\tau_1)\right)\right)_t=F_z(\tau_1)\ \ pro\ \ m<n,\tau_1<t, \tag{17}$$

$$\sum_{i=1}^{m}\left(K_{PU}(\tau_2)\cdot\overline{\delta}(\tau_2)+\frac{d}{d\tau_2}\left(\eta_{tPU}(\tau_2)\overline{\delta}(\tau_2)\right)\right)_t=F_o(\tau_2)\ \ pro\ \ m<n,\tau_2<t \tag{18}$$

$$\overline{\delta}(\tau_1)=\delta(\tau_1)-\frac{F_z(\tau_1)}{K_{oPU}}-\frac{1}{\eta_{tPU}}\int_0^{\tau_1}F_z(\tau_1)dt, \tag{19}$$

$$\overline{\delta}(\tau_2)=\delta(\tau_2)-\frac{F_o(\tau_2)}{K_{oPU}}-\frac{1}{\eta_{tPU}}\int_0^{\tau_2}F_o(\tau_2)dt, \tag{20}$$

where $F_z(\tau_1)$ describes stress force in time $\tau_1 < t$, $F_o(\tau_2)$ describes relieving force in time $\tau_2 < t$, $\overline{\delta}(\tau_1)$ describes the duration of the material compression, that is different in time during hysteresis (significantly longer, shorter, or negligible), among others due to resistance of the material compared with the relief time $\overline{\delta}(\tau_2)$, $K_{PU}(\tau_{1,2})$ is the immediate value of rigidity of the PU foam sample during compression, and stress relief $\eta_{tPU}(\tau_{1,2})$ is the immediate value of PU foam sample dampening during compression and stress relief.

The functional dependence of the total rigidity and total dampening of the structure can be consequently described.

$$K_{PU}(t)=\sum_{i=1}^{n}\left(\frac{\frac{\overline{\delta}(\tau_2)}{\tau_2}\cdot F_z+\frac{\overline{\delta}(\tau_1)}{\tau_1}\cdot F_o}{\left(\frac{\overline{\delta}(\tau_1)}{\tau_1}+\frac{\overline{\delta}(\tau_2)}{\tau_2}\right)\cdot\overline{\delta}(t)}\right)_t, \tag{21}$$

$$\eta_{tPU}(t)=\sum_{i=1}^{n}\left(\frac{\frac{\overline{\delta}(\tau_1)}{\tau_1}}{\left(\frac{\overline{\delta}(\tau_1)}{\tau_1}+\frac{\overline{\delta}(\tau_2)}{\tau_2}\right)\cdot\overline{\delta}(t)}\int_0^{t}(F_z(\tau_1)-F_o(\tau_2))dt\right)_t, \tag{22}$$

where $K_{PU}(t)$ describes total rigidity of the PU foam sample, and $\eta_{tPU}(t)$ describes total dampening of the sample.

Also through the work difference, it is possible to obtain the relation for the dissipated energy $\vartheta(t,\delta,T)$, which describes energy that can be absorbed by the material.

$$\vartheta(t,\delta,T)=\sum_{i=1}^{n}(W_z-W_o)_t=\sum_{i=1}^{n}\oint(F_z-F_o)_t dl, \tag{23}$$

where W_z, W_{od} describe work that the material does during compression and unloading.

Using this model, it is possible to describe creep suppleness $\Theta(t)$ in Eq. (24).

$$\Theta(t) = \frac{1}{E_0}(1 - e^{\frac{t}{\tau}}) + \sum_{i=1}^{m} \Theta(m) \cdot \left(1 - e^{\left(-\frac{t}{\tau}\right)^m}\right) \quad for \;\; m < n, \tau_2 < t, \tag{24}$$

where E_0 is the initial stiffness module.

Results of the n-parametric Tucket model expressed as the dependence of the tension on the transformation are shown in **Figure 17** where courses are in a very good agreement with the experiment. Correlation coefficient comparing between surveyed courses has a value of ~0.978. Certain difference is probably given by a fact that the rheological model does not include the structure morphology, i.e., the cell walls bend and from a certain phase of compression create friction between one another. According to Eqs. (21) and (22), it is possible to determine the course of rigidity and dampening of the PU foam sample (**Figure 18**).

Using appropriate relations, we can determine absolute value of deformation energy $E(\mu)$ or deformation work $W(\mu)$ that is necessary to apply to compress such structures. Fibrous structures are not conservative, therefore during the compression depending on the character of the deformation from the initial to final state, according to Ref. [18], it can be considered that

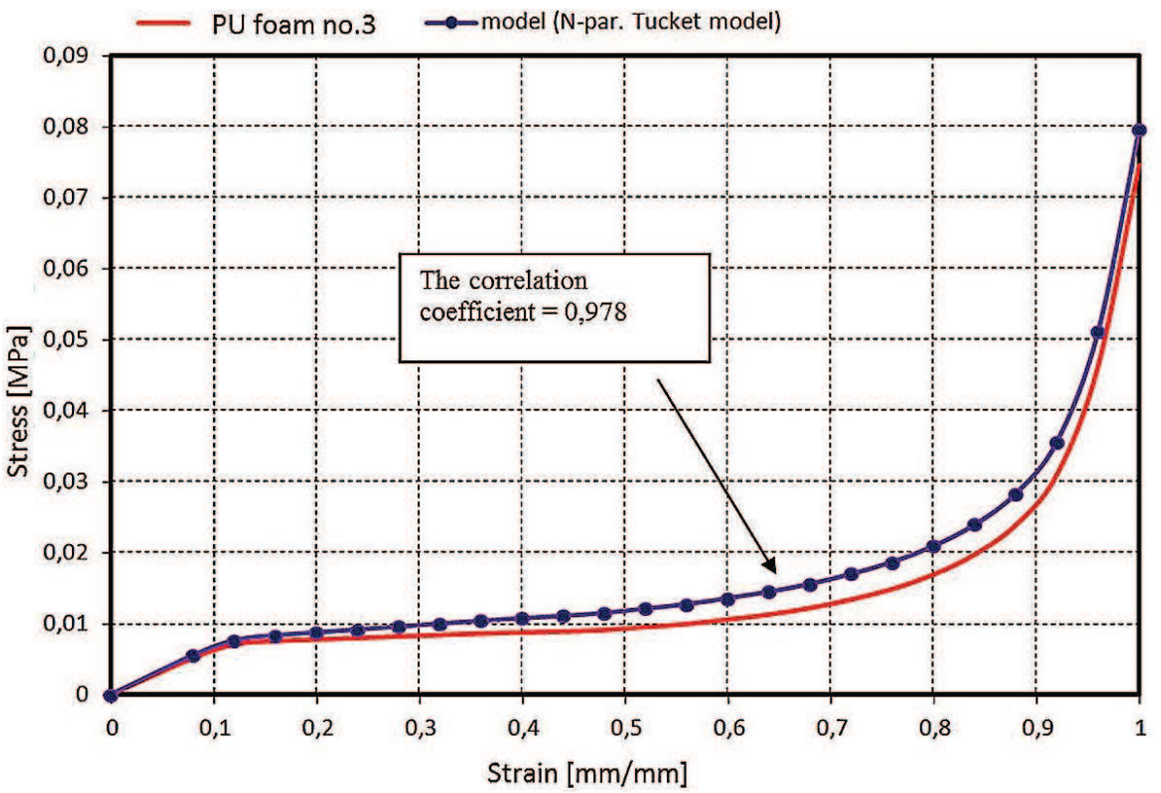

Figure 17. Comparison of nonlinear dependence of stress on strain of PU foam, experiment (line), n-Tucket n-parametric model (dotted line), and correlation coefficient 0.978.

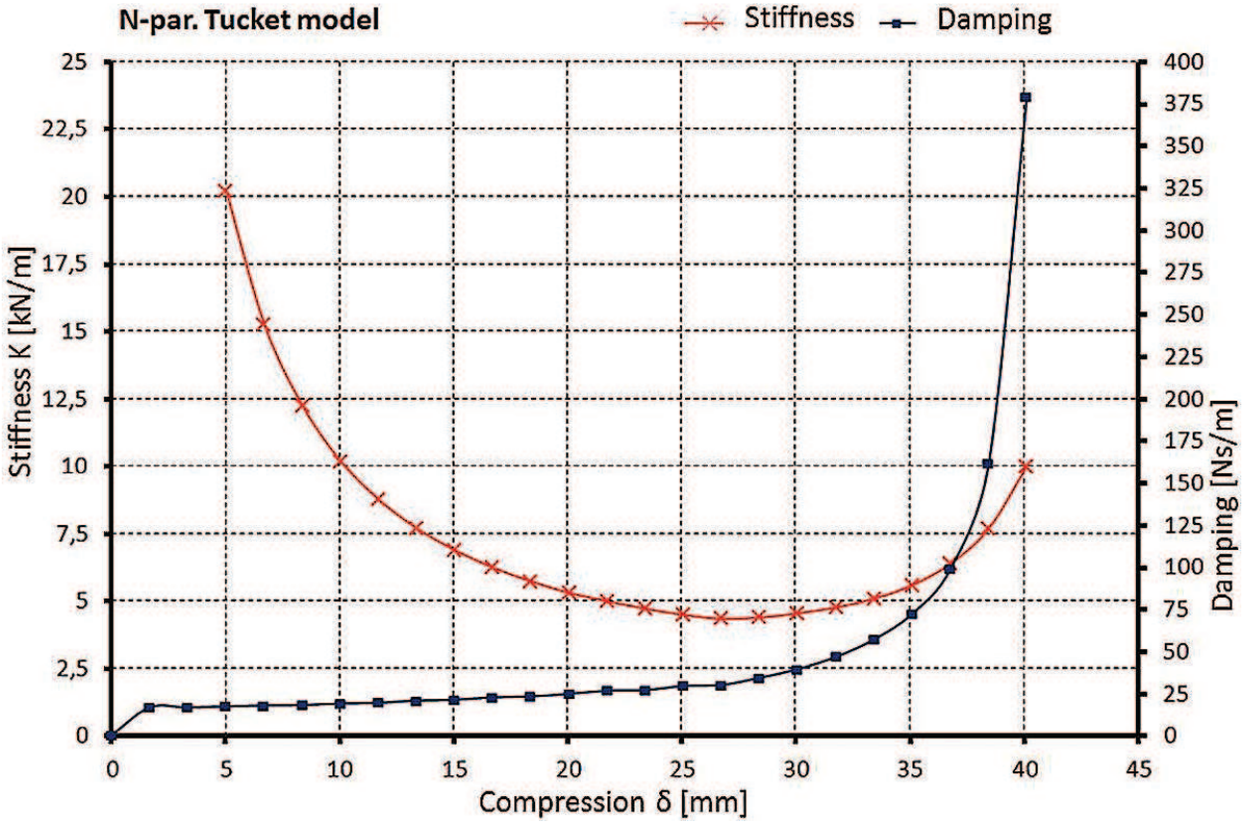

Figure 18. *N*-parametric Tucket model: course of stiffness and damping depending on compression.

elementary work growth dW used to compress structure is directly proportional to the elementary gain of the deformation energy dE according to the Eq. (25) where elementary energy gain is a total function differential $E(\mu) = E_\mu(\varepsilon_i)$, which can be described by Einstein summary convention according to Eq. (26). Deformation into individual directions ε_i is possible to further describe using the filling μ according to Eq. (25). It is then possible to gain derivation change (transformation) of the filling in dependence to the deformation ε_i as per Eq. (26).

$$dW(\mu) = CdE(\mu) \quad pro \quad C \geq 1, \tag{25}$$

$$dE = \frac{\partial E}{\partial \varepsilon_i} d\varepsilon_i \quad pro \quad i = 1, \ldots, 3, \tag{26}$$

$$\mu = \frac{V_V}{V_C} = \frac{V_V}{(1+\varepsilon_i)(1+\varepsilon_j)(1+\varepsilon_k)} = \frac{\mu_0}{(1+\varepsilon_i)(1+\varepsilon_j)(1+\varepsilon_k)} \tag{27}$$

$$\frac{\partial \mu}{\partial \varepsilon_i} = \frac{\partial}{\partial \varepsilon_i}\left[\frac{\mu_0}{(1+\varepsilon_i)(1+\varepsilon_j)(1+\varepsilon_k)}\right] = \frac{-\mu_0}{(1+\varepsilon_i)^2(1+\varepsilon_j)(1+\varepsilon_k)}, \tag{28}$$

where $W(\mu)$ is a deformation work ($W(\mu) = \int \sigma d\varepsilon$), C is a constant of proportionality, $\varepsilon_{i,j,k}$ describes deformation into the main direction of extension, and μ_0 is the initial filling, i.e. $\mu_0 = V_V$.

The structure creates resistance during deformation against the compression described by the distribution of Cauchy (real) stress tensor σ_{ii} related to the areas in the deformed continuum,

http://dx.doi.org/10.5772/intechopen.69700

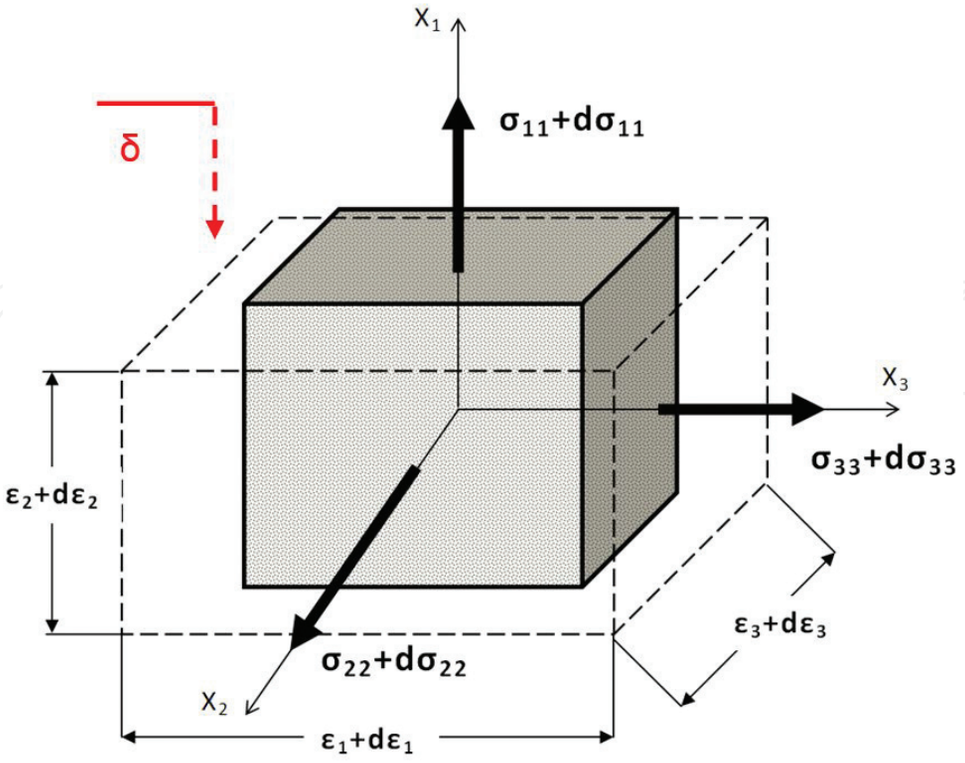

Figure 19. Elementary continuum of compressed structure.

which is well described in Ref. [19]. This is described in **Figure 19**, which shows base configuration of elementary continuum cube, where $\varepsilon_i = 0|_{t=t_0}$ transforms during increases in deformation into the deformed shape $\varepsilon_i \neq 0|_{t>t_0}$. Using Cauchy stress tensor σ_{ii}, it is possible to describe Eq. (25) by the sum of contributions to the main directions of deformation, which is given by Eq. (29). Total stress σ_{HMH} described by the von Mises hypothesis (Eq. (30)) based on normal parts of Cauchy stress tensor σ_{ii} simply describes the compression pressure p_k.

$$\sum_{i=1}^{3} \sigma_{ii} d\varepsilon_i = C \sum_{i=1}^{3} \frac{\partial E}{\partial \varepsilon_i} d\varepsilon_i \tag{29}$$

$$\sigma_{HMH} = \sqrt{\frac{1}{2}\left[(\sigma_{11} - \sigma_{22})^2 + (\sigma_{22} - \sigma_{33})^2 + (\sigma_{11} - \sigma_{33})^2\right]} \tag{30}$$

where σ_{HMH} is a total (reduced) tension according to the hypothesis HMH (Huber, von Mises, Hencky), $\sigma_{11}, \sigma_{22}, \sigma_{33}$ are the Cauchy stresses in the main directions of the basic coordinate system X_i.

3.8. Summary of the property analysis of selected PU foam samples

The property analysis of the chosen PU foam construction samples determined that the tested samples have a low-permeable shell caused by the filled structure in form, and inner structure is permeable. Depending on the specific weight ρ, which can move from 47 to 51 kg

m^{-3},the packing density Ψ (1) increases while influencing the average cell size of the material structure (**Table 1**). Cellular structure of the PU foam sample influences strain-stress curve during compression. Typical course is characterized by the initial rigidity depending on the strain rate, given stable area so-called plateau and the final steep exponential increase in force.

Mechanical properties are significantly influenced by the character of the cellular structure, and they can be summarized as follows:

- Deformation ε is the function of not only tension σ, but also time t, and in the examined area (up to 95 ± 3% transformation), it can be considered **reversible**.
- Material deformation is **dampened** by inner viscose resistances, i.e., dampening of the cellular structure, η_{tPU}, therefore cannot be realized immediately.
- The faster the deformation happens, the more intense the dampening effect of the material viscosity materializes, but also the air viscosity, which cannot be squeezed out of the cellular structure immediately and, therefore, manifests as an initial significant increase in rigidity (the slower the compression, the lower the initial rigidity → the initial rigidity is nearing the behavior of the so-called plateau).
- **Recovery** manifests (recovery—the ability to immediately recover after deformation) given viscoelastic properties determined by hysteresis.
- **Relaxation** manifests, i.e., decrease in tension in prestressed condition $\sigma(t)|_{z-konst} < \sigma(0)$
- **Creep** manifests, i.e., the growth in deformation under constant pressure $\varepsilon(t)|_{\sigma-konst} > \varepsilon(0)$
- Mathematic-physical description of PU foam mechanical properties can be described by a constitutive relations and by **rheologic models**, for example, modified n-parametric Tucket model according to which it is possible to express the coefficient of rigidity and dampening of PU foam.
- For a qualitative analysis of the PU foam during compression, or for wider knowledge of mechanical properties that cannot be sufficiently measured nor mathematically described (distribution of main tensions and transformation in individual directions, contact pressures), it is suitable to construct **model simulation** of mechanical properties in the setting of the finite element method.

4. Model simulations of mechanical properties of selected samples

The analysis and measurements of mechanical properties of PU foam samples are generally limited only to certain information, and therefore, it cannot tell us the immediate distribution of deformation and tension in the material structure. This is because the options for measurements are limited; options to place sensors and some properties cannot be well measured (for example, distribution of main tension and deformation of the cellular structure). In this case, a compilation

of appropriate model simulation according to the numerical method becomes a viable option. Programming a model simulation in FEM setting is the most significant to our purpose, but certain ways also offer other numerical methods, for example, method of discrete elements (MDE), method of boundary elements (BEM), or method of finite volume (FVM). The FEM method was used exclusively in this work. Mechanical compression of the selected PU foam samples creates many heterogeneous attributes in its inner structure, which change with the size of deformation, as was stated. While modeling such structures, Refs. [8, 20] agree that it is necessary to simplify or ignore certain characteristic attributes, and both state that a great problem of modeling non-linear attributes is mostly the description of the main tensions in short time differentiations $\Delta t = t_{i+1} - t_i$. The solution of peripheral problem of great deformations created by compression of the sample further lies not only in the correct input of peripheral conditions and material properties, but also in the construction of proposed net of finite elements. FEM programs are currently very well worked out and allow for the conversion of continuous problem solution to the final solution, where it is possible to suggest appropriate geometrically simple partial sub-regions (finite elements) for approximate solution in the preprocessor.

Let $\aleph \subset R^3$ is a continuous area of three-dimensional space. Their boundaries will be Γ, where Γ is the so-called Lipschitz boundary, and let an approximation of the selected basis functions are derived over each finite element with dimension l, because any continuous function may be represented by linear combinations of algebraic polynomials converging to a continuous solution i.e. $\lim_{l \to 0} \to \xi \approx 1$. Thus, FEM can be understood as a special type of a variation method using mathematical description of solved problem. Current substantial commercial FEM software (for example, Ansys, Abaqus, Permas, LS-Dyna, Marc, and PAM CRASH) allow to assemble and then solve the loading of nonlinear materials not only with viscoelastic properties using mathematical relationships based on continuum mechanics and rheological model (for example, Kelvin model, Maxwell model, and so on). Also they allow with sufficient accuracy the studying and modeling of qualitatively more complex problems such as contacts of two or more bodies (i.e., the interaction between the material and probe or human body).

4.1. Selection of suitable software for the assembly of FEM model

In this study for all model simulations, software PAM CRASH was selected. It is the FEM software from ESI-Group company (http://www.esi-group.com/) that is used for the study of nonlinear isotropic and anisotropic materials and contact problems in quasi-static and dynamic states. Similar to FEM software as LS-Dyna, Abaqus Explicit, and ANSYS Explicit. The basic principle of explicit methods is second Newton's law, which may be expressed in a matrix form by Eq. (31).

$$M \cdot \ddot{u} = F^E - F^I, \tag{31}$$

where M is a matrix of mass, $\ddot{u}$ is the acceleration matrix of node vectors, F^E is the matrix of the vector of external forces acting on the node, and F^I is a matrix of vectors of internal forces (volume forces).

The matrix of acceleration vectors, where the acceleration expresses second derivation of the searched (unknowns) displacements (Eq. (32)), can be obtained according to Eq. (31). Then, vector matrix of internal and external forces can be expressed by Eqs. (33) and (34).

$$\ddot{u} = M^{-1} \cdot F^E - F^I \tag{32}$$

$$F^I = \sum_{\varepsilon=1}^{N_\varepsilon} \left(\int_\Omega B^T \cdot \sigma_n d\Omega + F^{Hurg} + F^{kont} \right), \tag{33}$$

$$F^E = \sum_{\varepsilon=1}^{N_\varepsilon} \left(\int_{v_\varepsilon} \rho \cdot \kappa_{i\infty}^{\varepsilon} dv_\varepsilon + \int_{s_\varepsilon} \chi_i \cdot \vartheta_\infty^{\varepsilon} ds_\varepsilon \right) \tag{34}$$

where B is matrix of basic functions of the strain, F^{kont} is the vector of the contact forces, F^{Hurg} is a vector of hourglassing damping forces, σ_n is the matrix of acting stress in member, ρ is density of the member, κ_i is vector of volume forces, and χ_i is vector of surface forces.

Founded matrix of displacement vectors u (Eq. (36)) can be expressed by an integration of the acceleration $\ddot{u}$ or velocity of displacements $\dot{u}$ (Eq. (35)) in accordance with following formulas:

$$\dot{u} = \dot{u}_{t+\Delta t/2} = \dot{u}_{t-\Delta t/2} + \ddot{u}_t \cdot \frac{\Delta t_t + \Delta t_{t+\Delta t}}{2} \tag{35}$$

$$u = u_{t+\Delta t} = u_t + \dot{u}_{t+\Delta t/2} \cdot \Delta t_{t+\Delta t} \tag{36}$$

where u_t is a vector of instantaneous velocity and $u_{t-\Delta t}$ and $u_{t+\Delta t}$ are vectors of previous or subsequent displacements.

The software has sophisticated algorithms for complex nonlinear contacts [21], where ongoing simulation model is divided into a selected sequence of m-intervals (where $m \leq t$ and $m_{\min} = 1$). For each time step, the displacement vector u_t is calculated. This vector describes that in following time step, the origin geometry $A0$ is changed to current geometry $A_{t+\Delta t}$ in consequence of the change of displacement vector $u_{t+\Delta t}$ in Eq. (37).

$$A_{t+\Delta t} = A0 + u_{t+\Delta t} \tag{37}$$

In further steps, instantaneous Cauchy stress $\sigma_{t+\Delta t}$ can be expressed using constitutive relations according to Eq. (38) that the algorithm processor expresses as strain change of elements $d\varepsilon = \partial u / \partial X_i$ (i =1,.., 3). Subsequently, a new vector of internal forces for individual nodes is calculated. Variable $t + \Delta t$ is overwritten with t, and the calculation proceeds to the next step.

$$\sigma_{t+\Delta t} = f(\sigma_t, d\varepsilon), \tag{38}$$

The resulting simulation time step Δt is described with Eq. (39) and relates to the calculation time, which is proportional to the size of the smallest element $l_{\min}$, the square root of the material density ρ, and inversely proportional to the square root of elastic modulus E.

The advantage of the explicit method is an order of magnitude faster than explicit method, because the implicit method the time step becomes a quadratic function [21].

$$\Delta t \leq \Delta t^{krit} = l_{\min} \cdot \sqrt{\frac{\rho}{E}} \tag{39}$$

where Δt^{krit} expresses the minimal (critical) time step for the simulation.

Subsequently, the processor for viscoelastic structure expresses Cauchy stress σ_{ij} by the tensor of a nominal stress σ_{ij}^{nom}, which is inversely proportional to vectors extension λ_i (Eq. (40)) as described [22].

$$\sigma_{ij} = \frac{\sigma_{ij}^{nom}}{\lambda_i \cdot \lambda_k} \tag{40}$$

where λ_i expresses vectors of extension to the principal directions and λ_k is a permutation index.

4.2. FEM simulation of mechanical properties of selected samples of PU foam

Simulations were performed in FE software for sample of the PU foam sample. Simulations were performed for a complete assessment of the selected material because the experimental methods cannot give an explanation of behavior and change of the shape, especially under dynamic loading. Model simulations were performed in the following steps:

- an assembling of two models dynamically compressed between rigid plates without initial deformation,
- a creation of the appropriate finite element mesh of the model in preprocessor and import of data file into the environment of PAM CRASH,
- a defining of appropriate initial and boundary conditions,
- an assembly of a nonlinear material model of selected samples,
- evaluating and comparing of the results of simulations in postprocessor.
- assembling of two models dynamically compressed between rigid plates without initial deformation,
- FE model consists of three parts: the test specimen and two plates (moveable and rigid). For each part of the model, structured finite element mesh using a special software Altair 11.0 Hypermesh was created. The finite element mesh was then imported through a text file with the extension *.pc* to the software PAM CRASH. All input parameters of the simulation model (material properties, loads, experimental data, contacts etc.) can be entered and verified in the data file. Assembled FE model is shown in **Figure 20**. The environment of the text file is shown in **Figure 21**.

Applied types and sizes of elements that affect the final time step Δt of the model (Eq. (39)) are shown in **Table 3**.

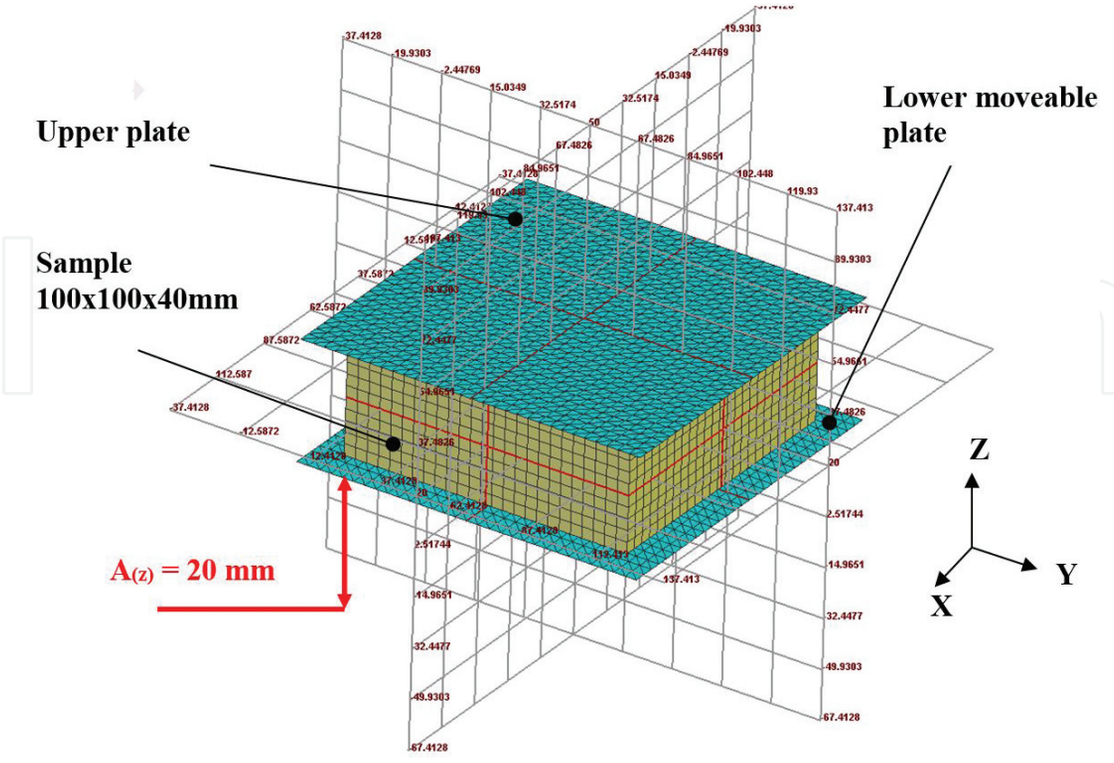

Figure 20. FEM model of sample dynamically compressed without the initial deformation.

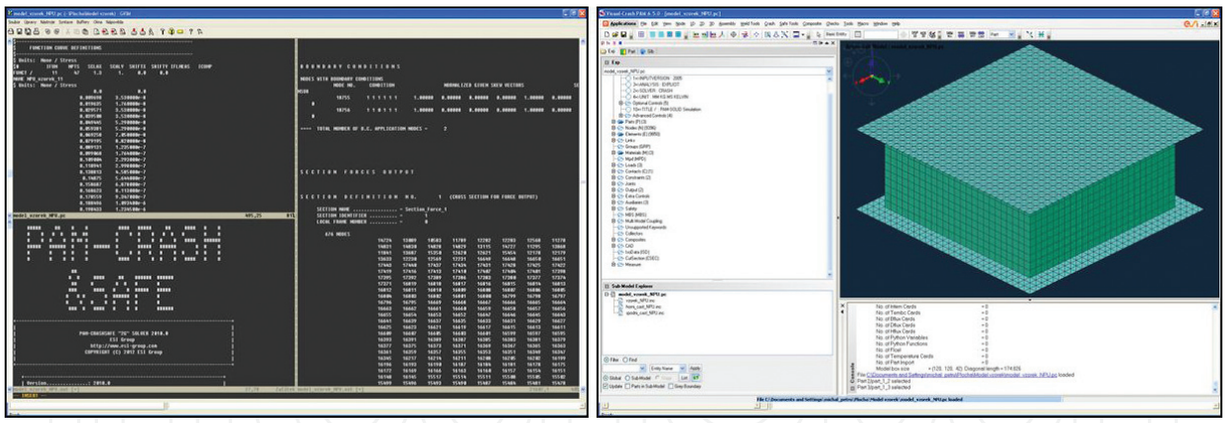

Figure 21. Modification of the input parameters in the FEM model dataset (left); visualization of the simulation model in PAM CRASH (right).

Model	Element type	Element size [mm]	Element number	Friction in contact	Distance between contacts [mm]	Time step Δt [s]
Rigid plates	2D shell	4	3600	0.1	0.5	5.297×10^{-1}
PU foam	3D solid	4	6250	0.1	0.5	0.1471×10^{-4}

Table 3. FEM model dynamically compressed sample.

http://dx.doi.org/10.5772/intechopen.69700

5. The initial and boundary conditions of the sample compressed with rigid plate

The initial and boundary conditions were defined as in the experiment. They can be summarized in the following points:

- geometric dimensions of the model sample are 100 × 100 × 40 mm,
- bottom plate was defined as perfectly rigid (so-called rigid body) with the translation in the vertical axis Z ($u_z \neq 0$, $u_{x,y} = 0$) with harmonic frequency and amplitude $A(z) = 20$ mm (i.e., 50% deformation) that is defined with Eq. (6),
- upper plate was again defined as rigid body without any translation (fixed) in all directions ($u_{x,y,z} = 0$), and
- contacts were defined between contact surfaces of the sample with plates (**Table 1**).

A solution of contact (Eq. (22)) between two or more parts in the explicit method consists in the fact that the surface of the acting component, so-called *Slave Area* (the plate), pushes on the surface of the second part, so-called *Master Area* (the sample), wherein the contact is calculated between the nodes of two bodies which are in the conjunction [23] (**Figure 22**).

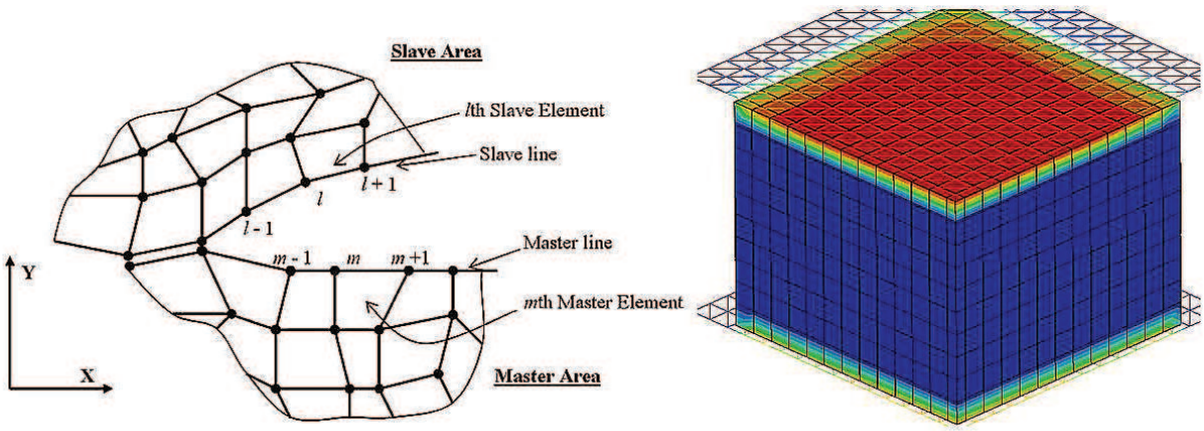

Figure 22. The principle of contact in the model simulations using explicit FEM scheme (left), and resulting model (right).

6. Material model assembling of selected PU foam

Material models in the PAM CRASH chosen to describe the nonlinear behavior of selected samples are prepared from material library, namely:

- Material model describing the mechanical behavior of PU foam has been defined through a nonlinear material model *45—General Nonlinear Strain Rate Dependent Foam with Optional Energy Absorption.* This material model has already been used and published, for example, in Refs. [3, 9, 12]. Its advantage is to especially allow to assess the influence of rigidity of polyurethane foams depending on the strain rate. The model is based on the rheological

behavior of the modified Kelvin model that allows to express Cauchy stress σ_i in the loading axis in accordance with Eq. (41).

$$\sigma_i = E \cdot \varepsilon_i(t) + \eta_t \cdot \dot{\varepsilon}_i(t), \tag{41}$$

where E is modulus of elasticity, $\varepsilon_i(t)$ and $\dot{\varepsilon}_i(t)$express the strain and strain rate in a single direction, and η_t is a damping of the material.

- Another suitable material can be material model 37—*Viscoelastic Ogden Rubber for Solid Elements*—which allows to describe not only viscoelastic but also hyperelastic material properties (suitable for the study of rubber, polymers, fibers, foams, etc.). This is based on the description of the functional dependence of the strain energy density $E(\lambda_1, \lambda_2, \lambda_3)$ defined by Eq. (42), expressing the energy that is required for the structure deformation. Practically, it is analogy to Eqs. (25) and (30).

$$E(\lambda_1, \lambda_2, \lambda_3) = \sum_{i=1}^{3} \frac{\mu_p}{\alpha_p} \cdot \left(\sum_{i=1}^{3} \lambda_i^{\alpha_\sigma} - 3 \right) \tag{42}$$

where $i = 1, \ldots, 3$, $E(\lambda_1, \lambda_2, \lambda_3)$is the strain energy density, μ_p and α_p are material constants, and let $\sum_{p=1}^{n} \frac{\mu_p \cdot \alpha_p}{2} = G$, where G is the shear modulus defined by Eq. (43), and $\lambda_i^{\alpha_\sigma}$vectors are elongation in principal directions.

$$G = \frac{F}{2 \cdot (1 + v)}, \tag{43}$$

where E is elastic modulus and v is Poisson's ratio.

Using strain energy $E(\lambda_1, \lambda_2, \lambda_3)$, the Cauchy stress in principal directions σ_i can be expressed in Eq. (44).

$$\sigma_i = p_k + \lambda_i^{\alpha_\sigma} \cdot \frac{\partial E(\lambda_1, \lambda_2, \lambda_3)}{\partial \lambda_i^{\alpha_\sigma}} \tag{44}$$

where p_k is compression stress.

The input material parameters of the simulation model are given in **Table 4**.

Part	Material model	Density [kg m^{-3}]	Initial module E [MPa]	Poisson ratio γ [–]	Damping coefficient
Rigid plates	Linear elastic	7850	210,000	0.3	–
PU foam	mat. 45	50.16	2.6	–	0.2

Table 4. Material properties of FEM model dynamically loaded sample.

http://dx.doi.org/10.5772/intechopen.69700

7. Results of simulations

The input signal and a material response are shown in **Figure 23**. The results of simulations for frequency 5 Hz are shown in **Figure 24**. In comparison with the real experiment, simulated values have a high correlation coefficient (0.961) up to 37.5% deformation (compression of 15 mm). The correlation coefficient between the model and the real measurement when compressed to 50% deformation exhibits a correlation of 0.932. The results of dynamically compressed samples against the rigid plate without the initial deformation with parameters according to **Table 4** are in good agreement with experiments.

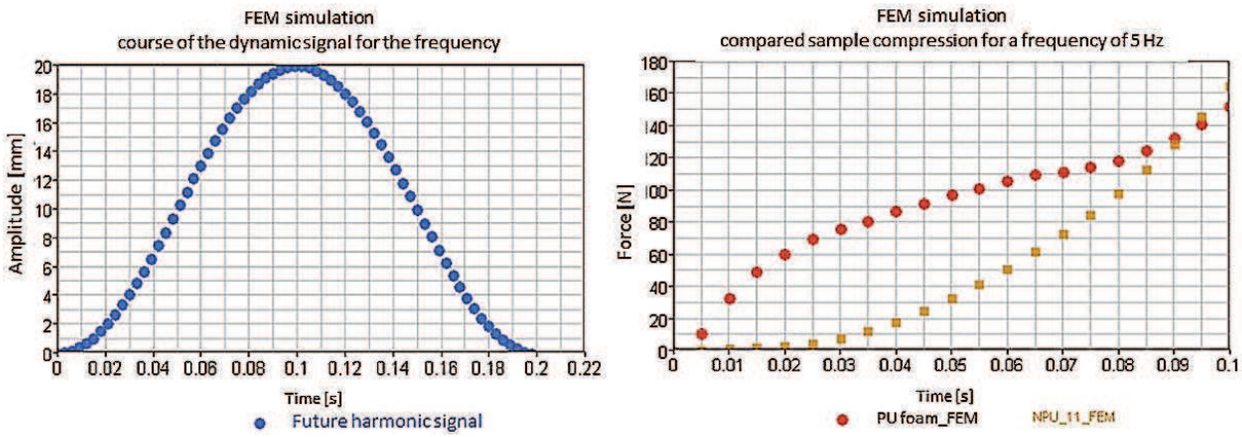

Figure 23. FEM model: excitation signal (left), and the response of the material on compression (right).

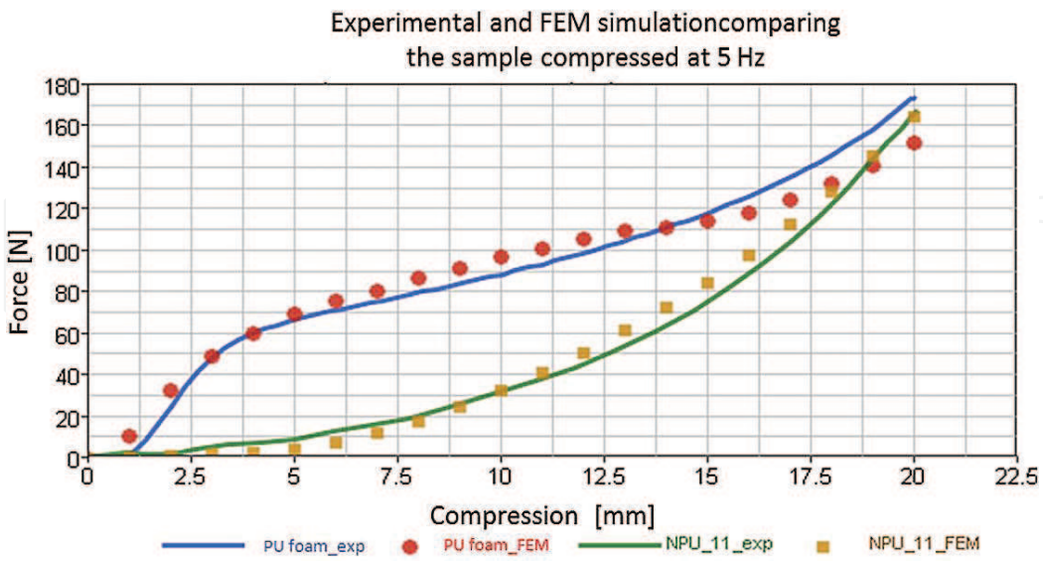

Figure 24. Comparison of the courses of experiment and FEM models.

The distribution of strain in the *X* and *Y* directions (plane perpendicular to the axis of compression) at a 37.5% deformation of the sample showed (**Figure 25**) that a sample of the PU foam in these directions is significantly deformed, because in these areas, there is highest stress. The maximum value of displacement vectors is 6404 mm, which is approximately 15% deformation of the sample. This leads to the fact that the structure is substantially pushed out from the sample. In contrast, non-polyurethane sample no. 11 is not practically in the plane perpendicular to the axis of compression deformed (**Figures 26–28**), because the maximum value of the displacement vectors is 0.034 mm.

Strain distribution also influences the value of the maximum principal stress during compression, as shown in **Figures 26–28**.

Results of the main stress shown in **Figure 28** indicate that material of the PU foam sample is pushed out already at 12.5% deformation. This phenomenon confirms that the PU foam with increasing strain rate increases the stiffness and the foam is pushed out. These results were further studied and tested in Refs. [3, 12]. The simulation of contact pressures has shown that the strain of the foam in directions perpendicular to the direction of compression leads to uneven stress distribution, which is reflected by the uneven distribution of contact pressures; however, these results cannot be obtained experimentally under dynamic loading. That is why

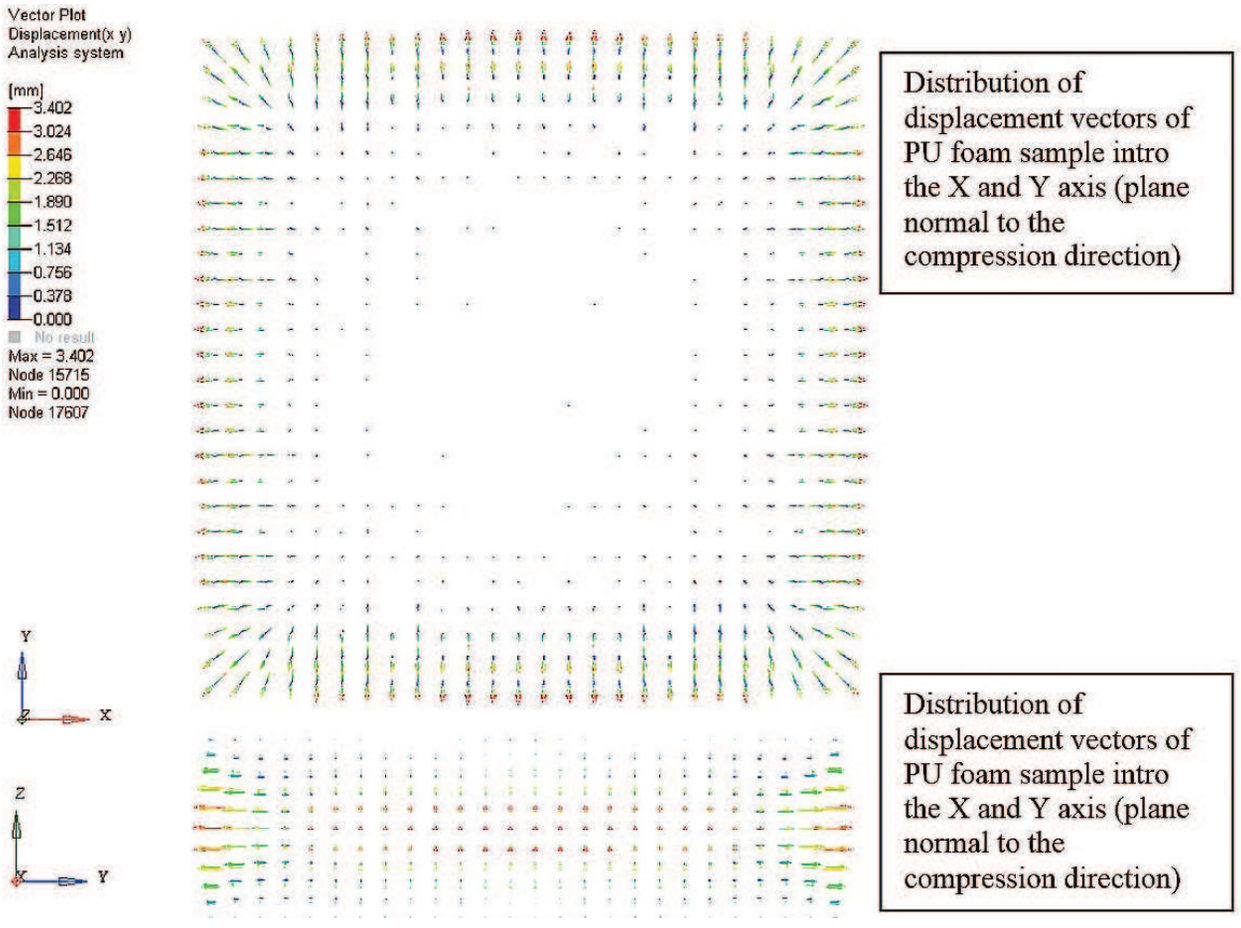

Figure 25. FEM model of PU foam sample, distribution of displacement vectors at 37.5% deformation.

http://dx.doi.org/10.5772/intechopen.69700

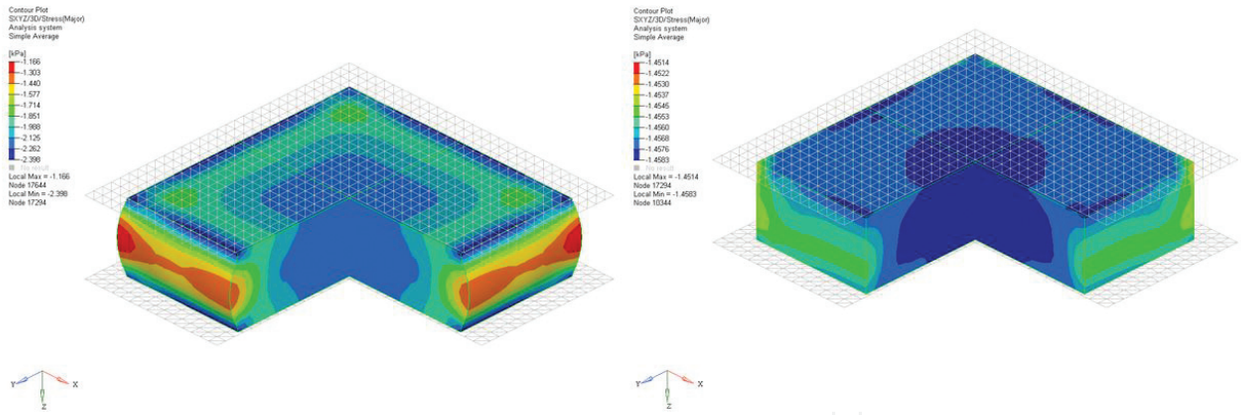

Figure 26. Deformation 37.5%: FEM model of PU foam sample.

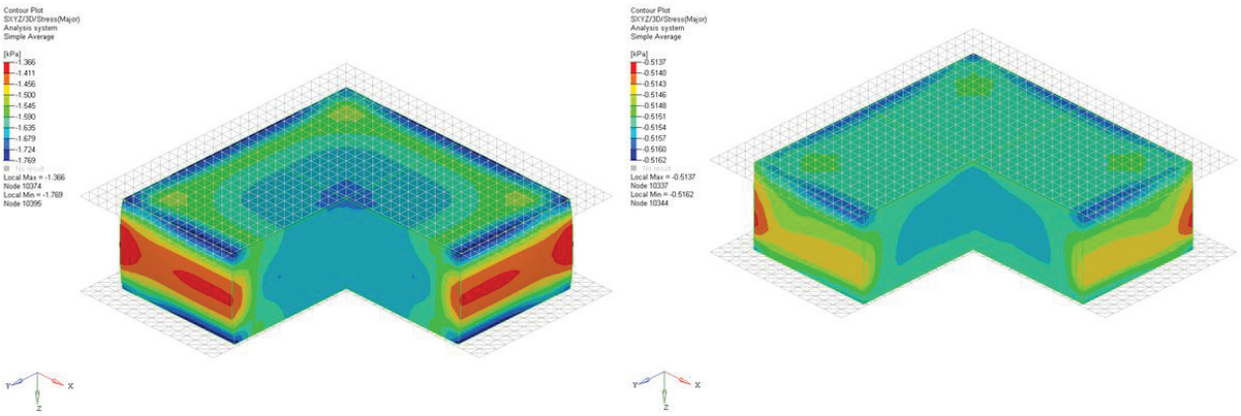

Figure 27. Deformation 25%: FEM model of PU foam sample.

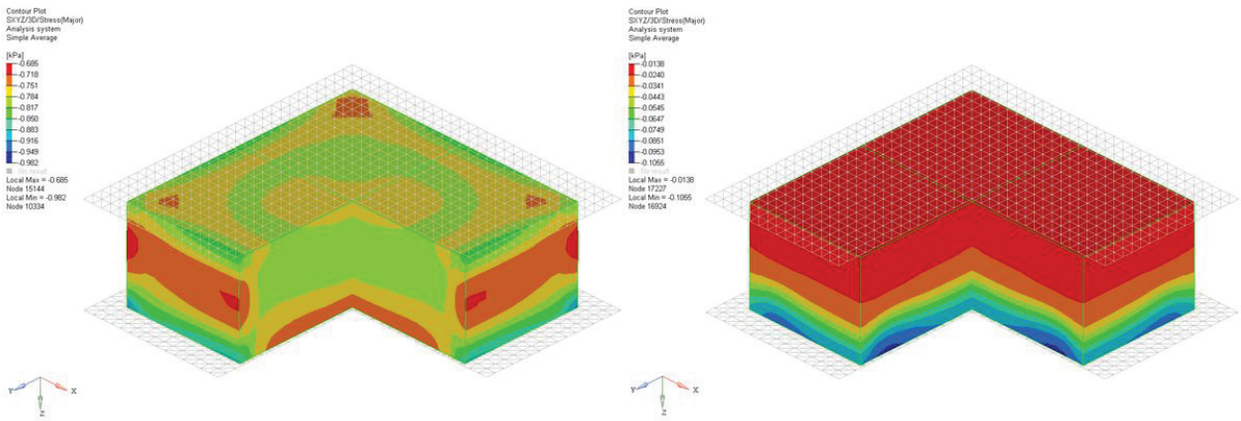

Figure 28. Deformation 12.5%: FEM model of PU foam sample.

the modeling is a suitable tool for obtaining of information that is not possible to achieve by the experiments (**Figure 29**).

The results of loading at frequency 5 Hz and 37.5% deformation are summarized in **Table 5**.

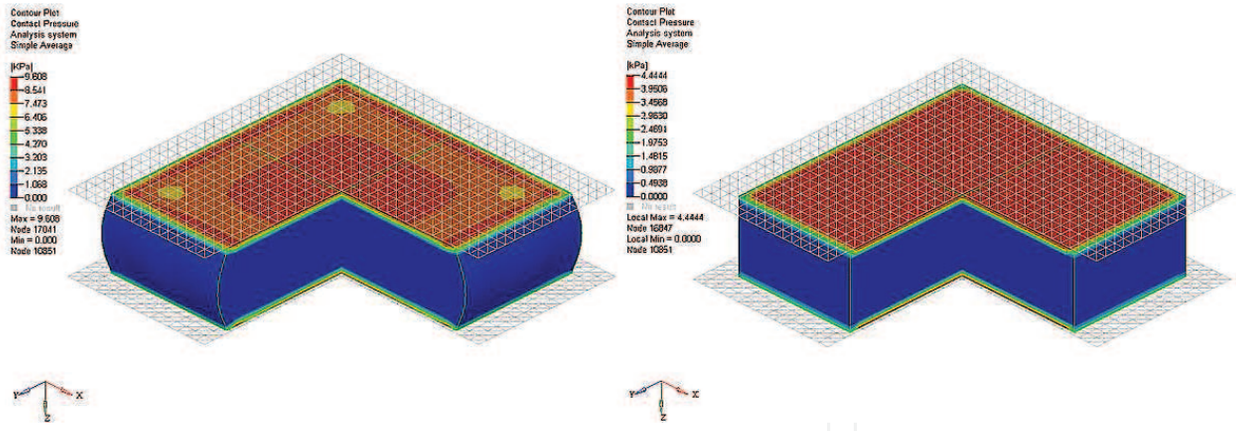

Figure 29. FEM model: comparison of contact pressures distribution at 37.5% deformation.

Sample	Deformation [%]	Principal stress [kPa]	Total stress [kPa]	Contact pressure [kPa]
PU foam	37.5	2.398	2.422	9.608

Table 5. Results of stress in dynamically compressed sample.

8. Conclusion

For static and dynamic measurements of samples, experimental devices were designed and implemented. Results showed that mechanical properties of PU foams are dependent on the strain rate, because the air in the initial stage cannot escape from the structure under dynamic loading, thus the air participates on the resulting foam properties. These results in increase of the main stress in the peripheral parts of the PU foam sample, as shown in the simulation of the sample loaded with harmonic signal. From the results of measurement of the relaxation, it was observed. Using the FEM simulation, the distribution of contact pressures was also compared. It was showed that the strain of the PU foam in directions perpendicular to the direction of compression leads to uneven stress distribution, which is reflected by the uneven distribution of contact pressures.

The described behavior influences properties of products containing PU foams. This behavior is significantly reflected in the construction of car seats. For example, headrests are used to capture the head in the rear impact (so-called whiplash). The energy absorption may be insufficient due to the setting of the headrest. If the backrest is fully inserted, a significant deflection of the spine in the area of the cervical vertebrae occurs, while if the headrest is correctly set, the spine is not deflected. Also, a dependence of material stiffness on strain rate has certain influence. The solution could be not only in the modification of the geometry and the anatomical design of the seat, but also in the change of the headrest stuff material which is not so dependent on the strain rate. The solution could be in a usage of foams with a highly porous structure and foams in the combination with fibrous structures that do not exhibit strong dependence of stiffness on the strain rate.

Furthermore, it has been shown that the PU foam is not capable to transmit tensile stresses. If the foam is under tensile stress, the stiffness will be very high with very low ability to deform. This means that low deformation and also the force cause a tearing of the cell structure. If the torn foam is further stressed, complete destruction occurs. This is especially important for mounting and assembling, such as inserting a seat foam, backrest, or mattress into the cover. This problem is further accentuated by relatively high surface friction of the foam to other materials. Therefore, it is suitable to use an interlayer that reduces the friction between the surfaces, e.g., interposed polyethylene film, which is removed after assembly or layer, which is inserted permanently. On the other hand, the foam that is already torn can transmit a pressure load without significant impact if the foam is placed in a cover or box that does not allow its distortion in a direction that is perpendicular to acting load.

Also, it has shown that molded polyurethane foam has a qualitatively different surface compared to the inner structure of the foam. The foam surface is closed, its porosity is very low, and its character approaches the integral foam. The surface also exhibits other mechanical properties, especially significantly higher stiffness in all kinds of loadings. This affects the load behavior, which is further influenced by the low permeability of the foam surface. As mentioned, the response to strain rate is a specific characteristic of foams and it is related to the cellular structure, especially its openness. If the surface is closed or only partially permeable to air, it influences the stiffness of the foam at a fast compression. The air is not able to immediately escape from the structure, and due to limited air compressibility, the rigidity of the foam increases. This can be seen especially in the first loading cycle, which is a crucial for impact during the crash when the human body is pushed into the foam. Therefore, it is appropriate to finish the surface in a suitable way, for example, by a grinding, perforating, grooving, etc. However, it should be noted that PU foam is invaluable material for static or quasi-static type of loadings. In particular, it is necessary to highlight behavior under compression loading. The strain-stress curve course is characterized by almost flat shape, so the force increases very slowly in large range of the deformation. This leads to the fact that the foam provides high comfort, because the foam very easily surrounds the body and reduces the contact pressure. This is not practically achievable for other materials and therefore PU foam is a material that is not easy to replace. Above all, PU foams exhibit balanced mechanical, physical, and thermal properties at low bulk densities and low weight. Also prduction costs are very low. That are the reasons for their use.

Author details

Michal Petrů[1]* and Ondřej Novák[2]

*Address all correspondence to: michal.petru@tul.cz

1 Institute for Nanomaterials, Advanced Technology and Innovation, Technical University of Liberec, Liberec, Czech Republic

2 Department of Nonwovens and Nanofibrous Material, Textile Faculty, Technical University of Liberec, Liberec, Czech Republic

References

[1] Mills NJ. Polymer Foams Handbook: Engineering and Biomechanics Applications and Design. Butterworth-Heinemann, UK; 2007

[2] Woldesenbet Em, Peter S. Volume fraction effect on high strain rate properties of syntactic foam composite. Journal of Material Science. 2009;**44**(6):1528–1539

[3] Petrů M, Novák O, Prášil L. Reduce of head injuries during whiplash by the help of materials with independent strain rate. Journal of Rehabilitation Medicine. 2011;**43** (Suppl. 50):28–29

[4] Cirkl D. Measurement of mechanical properties of polyurethane foam in vacuum. In: Academy of Science of the Czech Republic, editor. Dynamics of Machine; 6–7 February 2007; Prague. Prague: Academy of science of the Czech Republic; 2007

[5] Landrock AH. Handbook of Plastic Foams. USA: Library of Congress New Jersey; 1995

[6] Foye RL. Compression Strength of Unidirectional Composites. Columbus, USA: American Institute of Aeronautics and Astronautics, Structural Composites Group; 1996

[7] Bareš RA. Kompozitní materiály. SNTL Praha; 1988

[8] Mills NJ. The high strain mechanical response of wet Kelvin foams open cell foams. International Journal Solids Structure. 2007;**44**:51–65

[9] Petrů M, Petřík J. Systems to optimize comfort and developments of car seat. Acta Technica Corviniensis – Bulletin of Engineering, Annals of Faculty Engineering Hunedoara. 2009;**4**: 55–59

[10] Rush KC. Energy-absorbing characteristics of foamed polymers. Journal of Applied Polymer Science. 1970;**14**:1133–1147

[11] Neilsen MK, Morgan HS, Krieg RD. A Phenomenological Constitutive Model for Low Density Polyurethane Foams. SANDIA Report; 1987

[12] Petrů M, Novák O. Analysis and testing of mechanical properties of polyurethane foam and materials for nonpolyurethane car seat cushions. In: Praha CZU, editor. 4th International Mechanical Engineering Forum Prague; 2011; Prague. Prague: CZU Praha; 2011. pp. 135–149

[13] Rush KC. Load compression behavior of flexible foams. Journal of Applied Polymer Science. 1969;**13**:2297–2311

[14] Schwaber MD, Meinecke AE. Energy absorption in polymeric foams. II. Prediction of impact behavior from instron data for foams with rate-dependent modulus. Journal of Applied Polymer Science. 1971;**15**(10):2381–2393

[15] Nagy A, Ko WL, Lindholm US. Mechanical behavior of foamed materials under dynamic compression. Journal of Cellular Plastics. 1974;**10**(3):127–134

[16] Sinha SC, Mitchell JO, Lim GG, Chou CC. Constitutive modelling of energy absorbing foams. 1997; SAE paper no. 940880

[17] Zhang J, Kikuchi N, Li V, Yee A, Nusholtz G. Constitutive modeling of polymeric foam material subjected to dynamic crash loading. International Journal of Impact Engineering. 1988;**21**(5):369–386

[18] Liu Z, Zhang E, Ji Z. Simulation and experimental study of human Riding comfort in dynamic man-automobile system. Lecture Notes in Computer Science. 2008;**5314**(2008): 577–587

[19] Okrouhlík M, Höschl C, Plešek J, Pták S, Nadrchal J. Mechanika poddajných těles, numerická matematika a superpočítače. Praha: ÚT; 1997

[20] Kleiven S. A parametric study of energy absorbing foams for head injury prevention. In: Proceedings of the 20th International Technical Conference on the Enhanced Safety of Vehicles (ESV); 2007; Lyons France; 2007

[21] Belytschko T, Liu WK, Moran B. Nonlinear Finite Elements for Continua and Structures. Chichester, UK: John Wiley & Sons, Ltd; 2000

[22] Flanagan DP, Taylor LM. An accurate numerical algorithm for stress integration with finite rotations. Computer Methods in Applied Mechanics and Engineering. 1987;**62**:305–320

[23] Clinckemaillie J, Galbas HG, Kolp O, Thole CA, Vlachoutsis S. High scalability of parallel PAM-CRASH with a new contact search algorithm. Lecture Notes in Computer Science. 2000;**1823**:439–444

IntechOpen